a greaselike, soft solid that lacked a clear melting point. The product gave one spot on TLC (R_f 0.57, elution with the above solvent, detection by fluorescence quenching and by I_2 adsorption): ^{1}H NMR ($CDCl_3$) δ 0.88 (crude t, 6 H, 2 terminal CH_3's), 1.3 (broad s, 40 H, 2 $(CH_2)_4$'s and 2 $(CH_2)_6$'s), 1.52 (broad m, 4 H, 2 CH_2's β to carbonyls), 1.99 (broad m, 8 H, 4 allylic CH_2's), 2.22 (2 overlapping t's, 4 H, 2 CH_2's α to carbonyls), 3.28 (s, 6 H, $N^+(CH_3)_2$), ca. 4.0 and 4.4 (overlapping m's, 8 H, choline CH_2's and glyceryl CH_2's), 5.19 (m, 1 H, glyceryl CH), 5.33 (broad m, 4 H, vinyl), 5.42 (s, 2 H, benzyl CH_2), ca. 7.6 and 8.2 (m, 8 H, aromatic). Anal. Calcd for $C_{57}H_{91}N_2O_{12}P\cdot H_2O$: C, 65.49; H, 8.97; N, 2.68. Found: C, 65.26; H, 9.11; N, 2.39.

Preparation of Liposomes. Typically, 0.40 mL of a 5 mM functionalized phosphatidylcholine (6-F or 7-F) stock solution in chloroform was mixed with 2.80 mL of a 5 mM nonfunctionalized phosphatidylcholine solution (6-NF or 7-NF) in chloroform, and the chloroform was removed through evaporation under a gentle stream of nitrogen gas. This was followed by further drying under vacuum. To the film of the phosphatidylcholines thus obtained was added 20 mL of 10 mM BisTris buffer (containing 10 mM potassium chloride, with the pH adjusted to 6.0 with hydrochloric acid), and the mixture was sonicated at 55–60 W for 10 min under a nitrogen atmosphere. The temperature was controlled by a water bath at 55 °C for the 6-F/6-NF system and at room temperature for the 7-F/7-NF system. There resulted an almost clear solution that was filtered through a Millex membrane filter (pore size, 0.8 μm) and was then allowed to cool to room temperature if necessary. The liposome solution thus obtained was diluted with an equal volume of the BisTris buffer and employed in further experiments.

Kinetic Studies. Reactions were initiated in a UV cuvette by mixing the appropriate liposome preparation (6-F/6-NF or 7-F/7-NF) at pH 6 in BisTris buffer–KCl (see above) with 1 N aqueous NaOH solution at 25 °C to bring the pH to 12. Saponification of the benzoate began immediately and was followed at 400 nm while the *p*-nitrophenylate product absorption was monitored. The initial rapid exovesicular benzoate hydrolysis was followed by a second, slower, endovesicular hydrolysis (see Figure 1). At the end of a kinetic run, the pH was lowered to 10 by the addition of a drop of HCl solution. The solution was then warmed to 65 °C for 30 min to ensure total benzoate hydrolysis. The absorbance at this point was taken as the infinity titer (point X in Figure 1). The pseudo-first-order rate constants for the slow and fast hydrolyses were calculated from absorbance vs time data by computer analysis. Kinetic data are summarized in Table I.

Permeation Experiments. Liposomes functionalized with the *p*-nitrophenylate moiety were obtained after complete hydrolysis of 6-F/6-NF or 7-F/7-NF as described above. The pH of the liposome sample was then reduced to 6 by the addition of aqueous HCl, and the solution was warmed to 65 °C to equilibrate the inner and outer liposomal pH. The *p*-nitrophenol functionalized sample was then cooled to 25 °C, and the external pH was raised to 12 by the addition of 1 N NaOH. An instantaneous (exovesicular) deprotonation led to a "jump" in the 400-nm absorbance. This was followed by a time-dependent increase in absorption corresponding to endovesicular deprotonation.

Flip-Flop Studies. Typically, 40 mL of the 6-F/6-NF or 7-F/7-NF liposome solution was mixed with ca. 0.5 mL of 1 N aqueous NaOH solution to bring the pH to 12. After 30 min, the hydrolysis was stopped by the addition of ca. 0.5 mL of 1 N aqueous HCl, which brought the pH of the solution back to 6. Then 2 mL of the acidified liposome solution was placed in a UV cuvette and incubated in a water bath at a controlled temperature for a certain period of time. After the solution had been cooled to 25 °C, its pH was brought back to 12 by the addition of ca. 0.25 μL of the 1 N NaOH solution. This caused the immediate dissociation of protons from *p*-nitrophenol groups on the outer surface of the liposomal bilayer membrane. The process was monitored at 400 nm. When there had been any flip-flop of the cleavage-intact functionalized phosphatidylcholine molecules from the inner surface to the outer surface of the liposomes during the incubation, it was detected as a new rapid hydrolysis. After the completion of the new fast hydrolysis, if any, the sample was hydrolyzed at 65 °C, as described above, to obtain the total absorbance.

The extent of flip-flop was determined using eq 1, as described under Results. Pertinent data are summarized in Figures 2 and 3 and in Table I. Further details of our flip-flop protocol are discussed in ref 8.

Acknowledgment. We are grateful to the U.S. Army Research Office for financial support.

Aromatic Nitration with Electrophilic *N*-Nitropyridinium Cations. Transitory Charge-Transfer Complexes as Key Intermediates

E. K. Kim, K. Y. Lee, and J. K. Kochi*

Contribution from the Chemistry Department, University of Houston, Houston, Texas 77204-5641. *Received September 3, 1991*

Abstract: Electrophilic aromatic nitration of various arenes (ArH) is shown to be critically dependent on labile charge-transfer complexes derived from *N*-nitropyridinium cations. The electrophiles $XPyNO_2^+$, with X = CN, CO_2CH_3, Cl, H, CH_3, and OCH_3, form a highly graded series of electron acceptors that produce divers [ArH,$XPyNO_2^+$] complexes, with charge-transfer excitation energies ($h\nu_{CT}$) spanning a range of almost 50 kcal mol^{-1}. The latter underlie an equally broad spectrum of aromatic substrate selectivities from the different nitrating agents ($XPyNO_2^+$), but they all yield an isomeric product distribution from toluene that is singularly insensitive to the X substituent. The strong correlation of the nitration rates with the HOMO–LUMO gap in the [ArH,$XPyNO_2^+$] complex is presented (Scheme III) in the context of a stepwise process in which the charge-transfer activation process is cleanly decoupled from the product-determining step—as earlier defined by Olah's requirement of several discrete intermediates. This charge-transfer formulation thus provides a readily visualized as well as a unifying mechanistic basis for the striking comparison of $XPyNO_2^+$ with other nitrating agents, including the coordinatively unsaturated nitronium cation ($NO_2^+BF_4^-$), despite their highly differentiated reactivities.

Introduction

Nitration of various aromatic compounds is commonly carried out with nitric acid, either alone or in conjunction with Brønsted and Lewis acids.[1] Strong acids are particularly effective as catalysts for the steady-state production of the nitronium ion (NO_2^+) as the active electrophile.[2] A wide variety of other nitronium "carriers" YNO_2 have also been employed directly, with their nitrating activity generally paralleling the base (nucleofugal)

(1) (a) Feuer, H., Ed. *Chemistry of the Nitro and Nitroso Groups*; Wiley: New York, 1969. See also: Patai, S., Ed. *Chemistry of Amino, Nitroso and Nitro Compounds, Supplement F*; Wiley: New York, 1982. (b) Topchiev, A. V. *Nitration of Hydrocarbons*; Pergamon: London, 1959.

(2) Ingold, C. K. *Structure and Mechanism in Organic Chemistry*, 2nd ed.; Cornell University Press: Ithaca, NY, 1953; Chapter 6. See also: Taylor, R. *Electrophilic Aromatic Substitution*; Wiley: New York, 1990. De La Mare, P. B. D.; Ridd, J. H. *Aromatic Substitution, Nitration and Halogenation*; Butterworths: London, 1959.

0002-7863/92/1514-1756$03.00/0

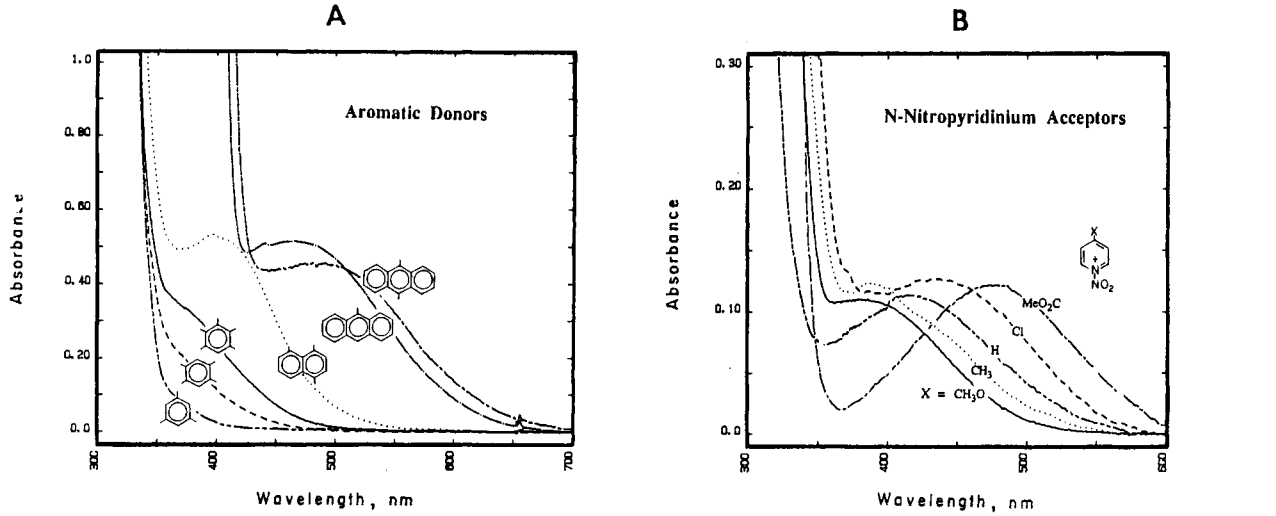

Figure 1. Charge-transfer spectra of (A) $MeOPyNO_2^+$ (0.03 M) with various aromatic donors (0.06 M as indicated) and (B) hexamethylbenzene (0.02 M) with various *N*-nitropyridinium acceptors (0.02 M as indicated) in acetonitrile.

strength of Y in the following order:[3] OH_2 (nitracidium ion) > Cl^- (nitryl chloride) > NO_3^- (dinitrogen pentoxide) > OAc^- (acetyl nitrate) > OH^- (nitric acid) > Py (*N*-nitropyridinium ion) > OCH_3^- (methyl nitrate) > $C(NO_2)_3^-$ (tetranitromethane).

As broadly conceived, the seminal mechanistic question in aromatic nitration focuses on the activation process(es) leading up to the well-established Wheland or σ-intermediate.[3,4] Therefore, if the conventional electrophilic addition of the coordinatively unsaturated nitronium cation to the aromatic compound (ArH) is important, i.e., eq 1,

$$ArH + NO_2^+ \longrightarrow Ar^+(H)(NO_2) \qquad (1)$$

by what means do the substitutionally inert and coordinatively *saturated* YNO_2 carriers effect nitration? In this connection it is important to recognize that the electrophilic agents NO_2^+ and YNO_2 are all electron deficient and thus capable of serving as effective electron acceptors in common with other nitro compounds.[5] A characteristic property of the latter is their ability to form electron donor–acceptor or EDA complexes with different types of electron-rich donors, including aromatic hydrocarbons:[6]

$$YNO_2 + ArH \underset{}{\overset{K_{EDA}}{\rightleftharpoons}} [YNO_2,ArH] \qquad (2)$$

Such nonbonded EDA complexes are also referred to as charge-transfer or CT complexes,[7] since they are often colored and show intermolecular absorption bands ($h\nu_{CT}$) that have been spectroscopically characterized by Mulliken.[8,9] The importance of charge-transfer complexes as intermediates in aromatic nitration with the nitronium ion was originally presented theoretically (without experimental support) by Brown[10] and by Nagakura and Tanaka.[11] Despite notable contributions by Olah and others,[12,13] this formulation has not been uniformly applied to nitration and related electrophilic aromatic substitutions.[2] Thus, it is noteworthy that the dual function of the nitrating agent has been separately known with tetranitromethane for a long time—as in the nitration of electron-rich arenes[14] and in the formation of EDA complexes with other aromatic donors.[15,16]

Since structural modifications are not readily achieved with tetranitromethane,[16] we have now turned our attention to the *N*-nitropyridinium acceptor, which can be prepared as a colorless crystalline salt,[17,18] free of any adventitious nitrosonium impurity, and used under essentially neutral conditions.[19] Furthermore, the reactivity of this reagent can be systematically varied, both with respect to electron demand as well as steric crowding,[17] by the judicious placement of suitable substituents on the heterocyclic moiety. Pertinent to the charge-transfer formulation will be our demonstration that these *N*-nitropyridinium cations in common with other nitrating agents are uniformly involved in the formation of a series of related aromatic EDA complexes prior to electrophilic aromatic nitration.[20] Furthermore, the use of substituted *N*-nitropyridinium derivatives allows a graded series of bases to be simultaneously generated in situ for the direct deprotonation of the Wheland intermediate in eq 1.

Results

I. Synthesis of Crystalline *N*-Nitropyridinium Salts. Pure nitronium tetrafluoroborate, free of any nitrosonium adulterant,[22] was converted to the crystalline *N*-nitropyridinium salt at −20 °C

(3) Olah, G. A.; Malhotra, R.; Narang, S. C. *Nitration*; VCH: New York, 1989.
(4) Wheland, G. W. *J. Am. Chem. Soc.* **1942**, *64*, 900.
(5) Chowdhury, S.; Kishi, H.; Dillow, G. W.; Kebarle, P. *Can. J. Chem.* **1989**, *67*, 603. See Feuer, H. in ref 1a.
(6) Andrews, L. J.; Keefer, R. M. *Molecular Complexes in Organic Chemistry*; Holden-Day: San Francisco, 1964. Briegleb, G. *Elektronen-Donator Komplexe*; Springer: Berlin, 1961.
(7) Foster, R. *Organic Charge-Transfer Complexes*; Academic: New York, 1969.
(8) Mulliken, R. S. *J. Am. Chem. Soc.* **1952**, *74*, 811.
(9) Mulliken, R. S.; Person, W. B. *Molecular Complexes*; Wiley: New York, 1969.
(10) Brown, R. D. *J. Chem. Soc.* **1959**, 2224 and 2232.
(11) Nagakura, S.; Tanaka, J. *J. Chem. Phys.* **1954**, *22*, 563. See also: Nagakura, S. *Tetrahedron (Suppl. 2)* **1963**, *19*, 361.
(12) Olah, G. A.; Kuhn, S. J.; Flood, S. H. *J. Am. Chem. Soc.* **1961**, *83*, 4571 and 4581.
(13) (a) Pedersen, E. B.; Petersen, T. E.; Torssell, K.; Lawesson, S.-O. *Tetrahedron* **1973**, *29*, 579. (b) Perrin, C. L. *J. Am. Chem. Soc.* **1977**, *99*, 5516. (c) For a recent summary, see: Ridd, J. H. *Chem. Soc. Rev.* **1991**, *20*, 149.
(14) (a) Schmidt, E.; Schumacker, R.; Bajor, N.; Wagner, A. *Chem. Ber.* **1922**, *55*, 1751. (b) Chaudhuri, J. N.; Basu, S. *J. Chem. Soc.* **1959**, 3085.
(15) (a) Ostromisslensky, I. *Zh. Russ. Fiz. Khim.* **1909**, *41*, 731. (b) Werner, A. *Ber.* **1909**, *42*, 4324. (c) Macbeth, A. K. *J. Chem. Soc.* **1915**, *107*, 1824. See also: Bruice, T. C.; Gregory, M. J.; Walters, S. L. *J. Am. Chem. Soc.* **1968**, *90*, 1612.
(16) (a) Altukhov, K. V.; Perekalin, V. V. *Russ. Chem. Rev.* **1976**, *45*, 1052. (b) Masnovi, J. M.; Kochi, J. K.; Hilinski, E. F.; Rentzepis, P. M. *J. Am. Chem. Soc.* **1986**, *108*, 1126.
(17) (a) Olah, G. A.; Olah, J. A.; Overchuk, N. A. *J. Org. Chem.* **1965**, *30*, 3373. (b) Olah, G. A.; Narang, S. C.; Olah, J. A.; Pearson, R. L.; Cupas, C. A. *J. Am. Chem. Soc.* **1980**, *102*, 3507.
(18) Jones, J.; Jones, J. *Tetrahedron Lett.* **1964**, 2117.
(19) Cupas, C. A.; Pearson, R. L. *J. Am. Chem. Soc.* **1968**, *90*, 4742.
(20) There is no indication in the published literature for the direct relationship between the formation of such EDA complexes as $[ArH,PyNO_2^+]$ and the nitration of benzene derivatives.[21] For a recent example, see: Duffy, J. L.; Laali, K. K. *J. Org. Chem.* **1991**, *56*, 3006.
(21) For naphthalenes, see: Sankararaman, S.; Kochi, J. K. *J. Chem. Soc., Perkin Trans. 2* **1991**, 1.
(22) Elsenbaumer, R. L. *J. Org. Chem.* **1988**, *53*, 437.

Table I. Charge-Transfer Spectra of Aromatic EDA Complexes with 4-X-Substituted *N*-Nitropyridinium Cations[a]

aromatic donor	IP[b] (eV)	λ_{CT} (nm)[c] X = CH_3O	CH_3	H	Cl[d]	CH_3O_2C[d]
mesitylene	8.42	332	334	340	344	360
durene	8.05	341	357	352	387	414
pentamethylbenzene	7.92	351	389	378	404	440
hexamethylbenzene	7.85	382	408	422	436	462
1,4-dimethylnaphthalene	7.78	410	414	425	455	502
9-methylanthracene	7.31	466	498	526	542	602
9,10-dimethylanthracene	7.14	524	526	534	542	658

[a] In CH_3CN at 0 °C, unless indicated otherwise. [b] From ref 27. [c] Maximum of charge-transfer band for *p*-X-substituted $PyNO_2^+$. [d] At −40 °C.

as described by Olah and co-workers.[17] Essentially the same procedure was also used to prepare the various analogues,

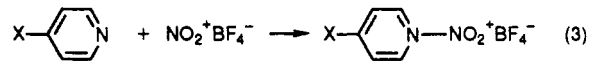

(3)

where X = methoxy, methyl, chloro, carbomethoxy, and cyano substituents, as colorless, extremely hygroscopic crystals. Similarly, nitronium hexachloroantimonate was converted to the pale yellow *N*-nitropyridinium salt and its 4-methoxy derivative.[23] All of the nitropyridinium salts were thermally stable, and they readily dissolved in rigorously purified acetonitrile to afford colorless solutions, provided sufficient care was exercised to avoid adventitious moisture. Since the *N*-nitropyridinium salts could not be prepared in situ without coloration,[24] all solutions were subsequently prepared from crystalline salts that were always manipulated in a moisture-free glovebox (see the Experimental Section).

II. Formation of Aromatic EDA Complexes with *N*-Nitropyridinium and Other Nitrating Agents. When *N*-nitropyridinium tetrafluoroborate was exposed to hexamethylbenzene dissolved in acetonitrile, the solution instantaneously took on a bright yellow coloration. The corresponding change in the electronic spectrum was observed as a new absorption band with $\lambda_{max} \approx 420$ nm by spectral (digital) subtraction of the low-energy tail absorption of the *N*-nitropyridinium salt alone.[25] Similar color changes occurred with nitric acid, acetyl nitrate, and tetranitromethane, and the corresponding spectral changes were not fundamentally distinguished from each other.[25,26] In every case, the new absorption was characterized by a long low-energy tail of a broad band of the type previously assigned by Mulliken to the charge-transfer transitions ($h\nu_{CT}$) in intermolecular EDA complexes.[9]

The systematic and quantitative study of the structural effects of the nitrating agent was carried out in acetonitrile solution with the related series of *N*-nitropyridinium cations with *p*-X substituents in eq 3. Thus, Figure 1A shows the characteristic red shift[6] of the new CT absorption band with the increasing strength of the aromatic donor, in the order mesitylene < durene < pentamethylbenzene < 1,4-dimethylnaphthalene < 9-methylanthracene < 9,10-dimethylanthracene, to accord with the decreasing ionization potentials listed in Table I.[27,28] Likewise, the new absorption band suffered a gradual blue shift[7] as the 4-substituent on nitropyridinium acceptor was systematically varied from X = carbomethoxy, chloro, hydrogen (unsubstituted), methyl, and methoxy (Figure 1B), as was visually apparent from the dramatic color changes from violet, red, orange, to yellow solutions.

Spectrophotometric analysis of the absorbance change of the new CT bands accompanying the variation in the concentration

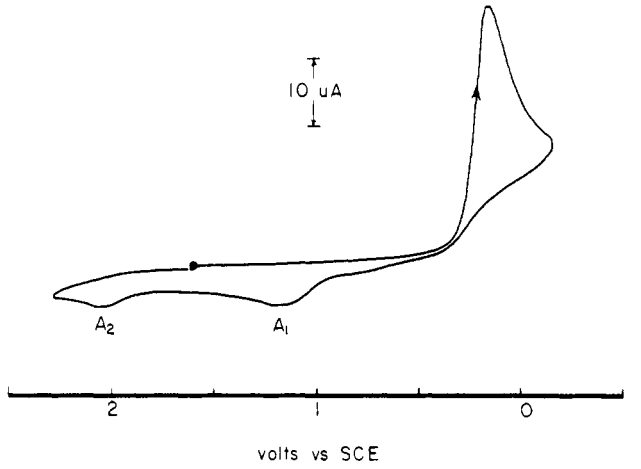

Figure 2. Cyclic voltammogram (initial negative scan at $v = 0.5$ V s^{-1}) of 5×10^{-3} M $PyNO_2^+BF_4^-$ in acetonitrile containing 0.1 M tetrabutylammonium hexafluorophosphate at 23 °C.

of the nitrating agents was carried out with the Benesi–Hildebrand procedure,[29]

$$\frac{[PyNO_2^+]}{A_{CT}} = \frac{1}{K_{EDA}\epsilon_{CT}[ArH]} + \frac{1}{\epsilon_{CT}} \quad (4)$$

for which the new absorbance (A_{CT}) was measured at various concentrations of the nitropyridinium acceptor in the presence of excess aromatic donor. The values of the formation constant K_{EDA} and extinction coefficient ϵ_{CT} of some representative EDA complexes are listed in Table II. The limited magnitudes of the formation constants $K_{EDA} \approx 1$ M^{-1}, evaluated for each of the nitrating agents, indicated that all of the aromatic complexes [YNO_2,ArH] were to be uniformly classified as weak.[30] Since such weak aromatic complexes have been successfully isolated as crystalline 1:1 salts,[31] numerous and varied attempts were made to isolate the analogous EDA complexes with *N*-nitropyridinium and its 4-methoxy derivative, either as the BF_4^- or $SbCl_6^-$ salt. Of the various benzene, naphthalene, and anthracene donors examined, we were finally able to isolate only yellow microcrystals of the 1:1 complexes of 1-methylnaphthalene and 1,4-dimethylnaphthalene with $MeOPyNO_2^+BF_4^-$, but they were both unsuitable for X-ray crystallography.

III. Quantitative Evaluation of *N*-Nitropyridinium Cations as Electron Acceptors. The strengths of cationic electron acceptors are most conveniently evaluated by the reduction potentials for the 1-electron process:[7]

$$PyNO_2^+ + e^- \overset{E^\circ_{red}}{\rightleftharpoons} PyNO_2^\bullet \quad (5)$$

Accordingly, the cathodic reductions of the series of *N*-nitropyridinium cations 4-$XPyNO_2^+$ in Table III were examined at 25 °C by cyclic voltammetry in acetonitrile solutions containing 0.1 M tetra-*n*-butylammonium hexafluorophosphate (TBAH) as the supporting electrolyte. Figure 2 shows the initial negative-scan cyclic voltammogram of $PyNO_2^+$ at a platinum electrode to consist of a well-defined cathodic wave at $E_p^c = 0.10$ V vs SCE at the scan rate of 0.5 V s^{-1}. The cathodic peak current corresponded to a 1.5-electron reduction of $PyNO_2^+$ by comparison with that from the ferrocenium standard.[32] The cathodic wave was highly irreversible since the coupled anodic wave was not observed, even

(23) Seel, F.; Nogradi, J.; Posse, R. *Z. Anorg. Allgem. Chem.* **1952**, *269*, 197.
(24) Arising from the nucleophilic ring opening of the nitropyridinium ion by free pyridine as described by Olah et al. in ref 17a.
(25) For the preliminary report, see: Figure 7 in Kochi, J. K. *Pure Appl. Chem.* **1991**, *63*, 262.
(26) The charge-transfer colors from $NO_2^+BF_4^-$ and either hexamethylbenzene, benzene, or toluene were too fleeting to be observed, even at −40 °C.
(27) Howell, J. O.; Goncalves, J. M.; Amatore, C.; Klasinc, L.; Wightman, R. M.; Kochi, J. K. *J. Am. Chem. Soc.* **1984**, *106*, 3968.
(28) Masnovi, J. M.; Seddon, E. A.; Kochi, J. K. *Can. J. Chem.* **1984**, *62*, 2552.
(29) Benesi, H. G.; Hildebrand, J. H. *J. Am. Chem. Soc.* **1949**, *71*, 2703. Person, W. B. *J. Am. Chem. Soc.* **1965**, *87*, 167.
(30) (a) Foster, R. In *Molecular Complexes*; Foster, R., Ed.; Crane, Russak: New York, 1974; Vol. 2, p 107 ff. (b) Hanna, M. W.; Lippert, J. L. In *Molecular Complexes*; Foster, R., Ed.; Crane, Russak: New York, 1973; Vol. 1, p 1 ff.
(31) For example, see: Wallis, J. M.; Kochi, J. K. *J. Am. Chem. Soc.* **1988**, *110*, 8207. Blackstock, S. C.; Lorand, J. P.; Kochi, J. K. *J. Org. Chem.* **1987**, *52*, 1451.
(32) Gagne, R. R.; Koval, C. A.; Lisensky, G. C. *Inorg. Chem.* **1980**, *19*, 2854.

Table II. Formation Constants of Aromatic EDA Complexes with Nitrating Agents[a]

aromatic donor (M)	YNO_2 (M)	λ_{mon}[b] (nm)	K_{EDA} (M^{-1})	ϵ_{CT} (M^{-1} cm^{-1})	ref
MeAnth[c] (0.04–0.2)	$CH_3OPyNO_2^+$ (0.014)	480	0.6	480	*d*
MeAnth[c] (0.04–0.2)	$PyNO_2^+$ (0.024)	510	1.2	180	*d*
MeAnth[c] (0.1–0.3)	$PyNO_2^+$ (0.01)	600	1.4		*e*
anthracene (0.04)	TNM (0.4)	500	0.3	300	*f*
Me_2Naph[g] (0.03–0.2)	$PyNO_2^+$ (0.02)	450	1.1	210	*h*
pentamethylbenzene (0.06–0.2)	$CH_3OPyNO_2^+$ (0.024)	420	0.6	190	*d*
durene (0.02–0.2)	$PyNO_2^+$ (0.02)	380	1.2	140	*d*
toluene (0.4–1.7)	$MeO_2CPyNO_2^+$ (0.02)	430	~4		*e*

[a] By Benesi–Hildebrand treatment in acetonitrile at 23 °C, unless indicated otherwise. [b] Monitoring wavelength. [c] 9-Methylanthracene. [d] This work. [e] From kinetic analysis; see text. [f] From ref 16b. [g] 1,4-dimethylnaphthalene. [h] From ref 21.

Table III. Reduction Potentials of *N*-Nitropyridinium Cations

X ($4\text{-}XPyNO_2^+BF_4^-$)	E_p^c (V vs SCE)[a]	pK_a[b]	ν_a (cm^{-1})[c]
CH_3O	−0.10	6.58	1698 (1687)
CH_3	0.06	6.03	1713 (1707)
H	0.10	5.21	1721 (1714)
Cl	0.25	3.83	1723 (1727)
CH_3O_2C	0.31	3.49	1729 (1729)
NC	0.50	1.86	1737 (1732)

[a] From the initial negative-scan cyclic voltammogram at v = 0.5 V s^{-1} in CH_3CN containing 0.1 M tetrabutylammonium hexafluorophosphate. [b] In water from ref 38. [c] Asymmetric nitro stretching frequencies in CH_3CN solution and in Nujol mull (in parentheses).

at scan rates exceeding 100 000 V s^{-1} using a platinum microelectrode.[33] Instead, two new anodic waves A_1 and A_2 are apparent in Figure 2 at E_p^a = 1.15 and 2.08 V on the return scan. The identical pair of anodic waves was observed in the initial negative-scan cyclic voltammetry of dinitrogen tetraoxide which is known to produce nitric oxide and nitrate,[34]

$$N_2O_4 + e^- \rightarrow NO + NO_3^- \quad (6)$$

Accordingly, the overall stoichiometry for the cathodic reduction of nitropyridinium ion is given as

$$2PyNO_2^+ + 3e^- \rightarrow NO + NO_3^- + 2Py \quad (7)$$

Such an electrode process followed from an initial electron transfer to afford an unstable nitropyridinyl radical[35]

$$PyNO_2^+ + e^- \rightarrow PyNO_2^{\bullet} \xrightarrow{\text{fast}} Py + NO_2 \quad (8)$$

and the subsequent dimerization of NO_2 followed by reduction. The latter are facile[36] and thus tantamount to the conversion of N_2O_4 in eq 6. When the fragmentation of the nitropyridinyl radical is rapid, the initial electron transfer in eq 8 is totally irreversible, and the trend in the peak potentials E_p^c will parallel the reversible reduction potential (see eq 5).[37] Indeed the linear correlation in Figure 3 establishes the direct bearing of the peak potentials E_p^c for various nitropyridinium ions on the thermodynamic stabilities of the corresponding hydropyridinium ions, as measured by their pK_a values.[38] The slope of the linear correlation in Figure 3 is −2.01 when both are expressed in the same energy units. Accordingly, the E_p^c values in Table III are to be taken as reliable measures of the acceptor strengths of various *N*-nitropyridinium cations.

IV. Aromatic Nitration with *N*-Nitropyridinium Acceptors. Products and Stoichiometry. The charge-transfer colors persisted for varying lengths of time, which depended on the particular combination of the arene donor and the nitropyridinium acceptor.

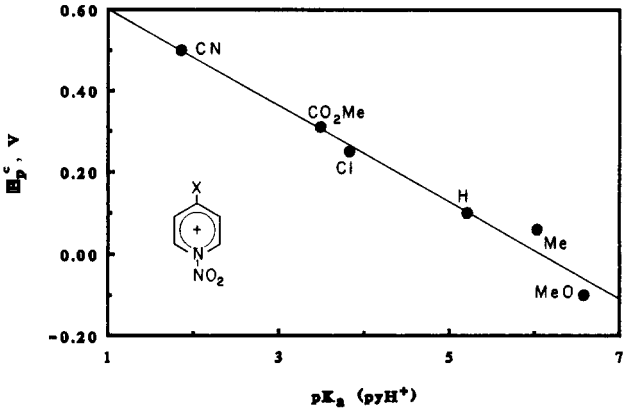

Figure 3. Electron acceptor properties of *N*-nitropyridinium cations ($XPyNO_2^+$) as measured by their E_p^c values in relationship to the thermodynamic stabilities of the corresponding hydropyridinium cations ($XPyH^+$) as evaluated by their pK_a values.

For example, the yellow color immediately attendant upon the mixing of $PyNO_2^+$ and benzene in acetonitrile was observed for about a day, whereas the orange solution from durene was bleached within 3 h. Under the same conditions, the charge-transfer color from durene and the carbomethoxy derivative of $PyNO_2^+$ was discharged within 60 s at room temperature, and it was only fleetingly observed as an orange flash with the cyano analogue. In each case, the loss of charge-transfer color was accompanied by the appearance of nitration products. Thus, the yellow solution of benzene and $MeO_2CPyNO_2^+$ was bleached within 10 min at 25 °C, and upon immediate workup it yielded nitrobenzene in 91% yield. Similarly, the transient CT color of the benzene (0.18 mmol) complex with $NCPyNO_2^+$ (0.13 mmol) in nitromethane was discharged within 1 min, and the ^1H NMR spectrum of the bleached solution indicated the presence of nitrobenzene (0.12 mmol) and $NCPyH^+$ (0.13 mmol), together with unreacted benzene (0.05 mmol). Accordingly, the aromatic nitration proceeded with the simple stoichiometry:

$$C_6H_6 + XPyNO_2^+ \rightarrow C_6H_5NO_2 + XPyH^+ \quad (9)$$

Similarly, the yellow solution of toluene and $NCPyNO_2^+$ afforded high yields of a mixture of the isomeric nitrotoluenes, the composition of which (*o*:*m*:*p* = 64:4:32) was essentially independent of the nitrating agent and the temperature, as indicated in Table IV.

Aromatic nitration by various nitropyridinium acceptors was also effective with other monosubstituted benzenes, such as anisole, chlorobenzene, bromobenzene, *tert*-butylbenzene, and benzotrifluoride (Table V). These aromatic donors were specifically chosen for the distinctive products and widely varying isomeric compositions that have been obtained with various nitrating agents.[3] For example, the consistently high incidence of the ortho-nitration of anisole with $MeOPyNO_2^+$ and $MeO_2CPyNO_2^+$ at 60 and 23 °C, respectively, in Table V (entries 11 and 12) mirrored that previously observed with acetyl and benzoyl nitrate[39]

(33) Compare: Kuchynka, D. J.; Kochi, J. K. *Inorg. Chem.* **1989**, *28*, 855.
(34) Bontempelli, G.; Mazzocchin, G. A.; Magno, F. *J. Electroanal. Chem.* **1974**, *55*, 91.
(35) On the basis of the fast-scan cyclic voltammetry,[33] the lifetime of the nitropyridinyl radical is estimated to be $\tau < 10^{-7}$ s.
(36) (a) Lee, K. Y.; Amatore, C.; Kochi, J. K. *J. Phys. Chem.* **1991**, *95*, 1285. (b) Redmond, T. F.; Wayland, B. B. *J. Phys. Chem.* **1968**, *72*, 1626.
(37) (a) Bard, A. J.; Faulkner, L. R. *Electrochemical Methods*; Wiley: New York, 1980; p 222 ff. (b) Compare: Klingler, R. J.; Kochi, J. K. *J. Am. Chem. Soc.* **1980**, *102*, 4790.
(38) Determined in water: Fischer, A.; Galloway, W. J.; Vaughan, J. *J. Chem. Soc.* **1964**, 3591.
(39) See: Schofield, K. *Aromatic Nitration*; Cambridge University Press: Cambridge, 1980; p 243.

Table IV. Toluene Nitration with $XPyNO_2^+$ and Other Nitrating Agents[a]

$XPyNO_2^+BF_4^-$ X	$XPyNO_2^+BF_4^-$ μmol	toluene (μmol)	nitrotoluene (μmol)[b] ortho	meta	para	conv (%)	temp/time (°C/h)
CH_3O	48	120	2.8 (61)	0.26 (6)	1.5 (33)	9.5	50/38
CH_3	49	94	1.5 (66)		0.73 (33)	4.5	23/56
H	76	190	34 (62)	2.5 (5)	18 (33)	72	23/45
Cl	61	122	24 (64)	1.5 (4)	12 (32)	74	23/3
CH_3O_2C	74	190	39 (62)	2.4 (4)	21 (34)	84	23/2
NC	100	230	47 (64)	3 (4)	23 (32)	73	23/3.5
NC	66	190	11.5 (72)	0.34 (2)	4.1 (26)	24	−17/24
$NO^+PF_6^-/O_2$	630	1200	100 (63)	6 (4)	52 (33)	25	3 °C[c]
$NO_2^+BF_4^-$	270	470	113 (55)	0.96 (0.5)	93 (45)	76	−78/12[d]
$NO_2^+BF_4^-$	290	470	167 (59)	6.6 (2)	111 (39)	97	23/0.16[d]

[a] In acetonitrile unless indicated otherwise. [b] Isomer composition (%) in parentheses. [c] In nitromethane from ref 90c. [d] In dichloromethane.

Table V. Nitration of Monosubstituted Benzenes with $XPyNO_2^+$[a]

$XPyNO_2^+BF_4^-$ X	$XPyNO_2^+BF_4^-$ μmol	SC_6H_5 S	SC_6H_5 μmol	$SC_6H_4NO_2$ (μmol)[b] ortho	meta	para	conv (%)	temp/time (°C/h)
CH_3O	60	Cl	98	2.4 (29)	0.2 (2)	5.7 (69)	14[d]	60/24
MeO_2C	50	Cl	118	6.2 (28)	0.3 (1)	16 (71)	45	23/1
c	580	Cl	1200	38 (29)	3 (2)	91 (69)	23	
CH_3O	34	Br	276		0.13 (9)	1.24 (91)	7[e]	60/120
MeO_2C	60	Br	190		0.17 (1)	12 (99)	21[f]	23/20
CH_3O	33	CF_3	164	0.12 (28)	0.26 (61)	0.05 (11)	1.3	60/72
CH_3O	60	*t*-Bu	123	3.8 (13)	4.3 (15)	20.8 (72)	48[h]	60/22
MeO_2C	84	*t*-Bu	170	10 (12)	12 (14)	63 (74)	100[i]	23/2
CN	49	*t*-Bu	100	2.6 (11)	3.4 (14)	18 (75)	50[j]	23/3
g	340	*t*-Bu	745	23.7 (12)	29.1 (15)	142 (73)	57[k]	23/1
CH_3O	60	CH_3O	120	13 (68)		6 (32)	30	60/21
MeO_2C	86	CH_3O	176	61 (71)		25 (29)	100	23/1.5

[a] In acetonitrile. [b] Isomer distribution (%) in parentheses. [c] $NO^+PF_6^-/O_2$ from ref 90c. [d] $MeOPyH^+BF_4^-$ (0.018) also found by ^1H NMR analysis. [e] $MeOPyH^+$ (0.033), 1,4-dibromobenzene (9×10^{-4}), and 1,3-dibromobenzene (1×10^{-4}) were also found. [f] 1,4-Dibromobenzene (6×10^{-4}). [g] $NO_2^+BF_4^-$. [h] $PhNO_2$ (3×10^{-4}), 1,3-di-*tert*-butylbenzene (4×10^{-4}), and 1,4-di-*tert*-butylbenzene (3×10^{-4}). [i] MeO_2CPyH^+ (0.063), $PhNO_2$ (2×10^{-4}), 1,3-di-*tert*-butylbenzene (1×10^{-4}), and 1,4-di-*tert*-butylbenzene (2×10^{-4}). [j] 1,3-Di-*tert*-butylbenzene (5×10^{-4}) and 1,4-di-*tert*-butylbenzene (4×10^{-4}). [k] $PhNO_2$ (4×10^{-4}), 1,3-di-*tert*-butylbenzene (5×10^{-4}), and 1,4-di-*tert*-butylbenzene (4×10^{-4}). For the footnotes, the quantities in parentheses are in units of micromoles.

Table VI. Trans Alkylation of *tert*-Butyl Groups during Aromatic Nitration with $XPyNO_2^+$[a]

aromatic donor (μmol)	$XPyNO_2^+BF_4^-$ X	$XPyNO_2^+BF_4^-$ μmol	products (μmol) $(t\text{-Bu})_2C_6H_3NO_2$	$t\text{-Bu}C_6H_4NO_2$	$t\text{-Bu}_nC_6H_{6-n}$
1,4-$(t\text{-Bu})_2C_6H_4$ (168)	CH_3O	24[b]	11[c]	3.8[d]	2.5[e]
1,4-$(t\text{-Bu})_2C_6H_4$ (121)	CH_3O_2C	68	43[c]	14.7[d]	1.1[f]
1,3-$(t\text{-Bu})_2C_6H_4$ (90)	CH_3O_2C	68	60[g]	*h*	

[a] In acetonitrile at 23 °C, unless indicated otherwise. [b] At 60 °C. [c] 1,4-$Bu_2C_6H_3NO_2$. [d] 4-*t*-$BuC_6H_4NO_2$. [e] Includes *t*-BuC_6H_5 (1.5), 1,3-$(t\text{-Bu})_2C_6H_4$ (1.0), and 1,2,4-$(t\text{-Bu})_3C_6H_3$ (0.9). [f] Includes *t*-BuC_6H_5 (0.7), 1,3-$(t\text{-Bu})_2C_6H_4$ (0.2), and 1,2,4-$(t\text{-Bu})_3C_6H_3$ (0.2). [g] Mixtures of 2-, 5-, and 6-nitro isomers of 1,3-$(t\text{-Bu})_2C_6H_3NO_2$. [h] Recovered 1,3-$(t\text{-Bu})_2C_6H_4$ (25.3). For the footnotes, the quantities in parentheses are in units of micromoles.

and nitronium tetrafluoroborate,[40] but these results contrasted with the predominance of *p*-nitroanisole using the mixed acid (HNO_3–H_2SO_4) in the presence of nitrosonium ion.[41] Although the nitrations of chlorobenzene with $MeOPyNO_2^+$, $MeO_2CPyNO_2^+$, and NO_2^+ all proceeded smoothly to the isomeric nitrochlorobenzenes (entries 1–3), bromobenzene afforded mainly *p*-bromonitrobenzene (no ortho isomer), together with small but distinctive amounts of the trans-bromination products 1,3- and 1,4-dibromobenzene.[42] Similarly, the nitration of *tert*-butylbenzene with $MeOPyNO_2^+$, $MeO_2CPyNO_2^+$, $NCPyNO_2^+$, and NO_2^+ yielded (entries 7–10) 1,3- and 1,4-di-*tert*-butylbenzene and nitrobenzene, together with high yields of the *tert*-butylnitrobenzenes with the usual isomer distribution.[43] Such side products provided useful insight into the nitration properties of the nitropyridinium acceptors, as presented for the individual aromatic donors below.

A. Transalkylation was the dominant process[44] in the nitration of 1,4-di-*tert*-butylbenzene, as shown in Table VI by the significant amounts of 1,2,4-tri-*tert*-butylbenzene, 1,3-di-*tert*-butylbenzene, and *tert*-butylbenzene obtained with $MeOPyNO_2^+$ and $MeO_2CPyNO_2^+$ at 60 and 23 °C, respectively (eq 10). By comparison, the isomeric 1,3-di-*tert*-butylbenzene underwent nitration exclusively on the ring, and no other products were detected.

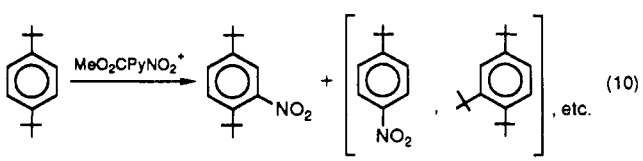

(10)

B. Side chain substitution and oxidation were extensive when the polymethylbenzenes, durene, and pentamethylbenzene (but not mesitylene) were treated with various nitropyridinium ac-

(40) Kovacic, P.; Hiller, J. J., Jr. *J. Org. Chem.* **1965**, *30*, 2871.
(41) Griffiths, P. H.; Walkey, W. A.; Watson, H. B. *J. Chem. Soc.* **1934**, 631. Bunton, C. A.; Minkoff, G. J.; Reed, R. I. *J. Chem. Soc.* **1947**, 1416. See Schofield in ref 39, pp 253–254.
(42) See: Moodie, R. B.; Schofield, K.; Weston, J. B. *J. Chem. Soc., Perkin Trans. 2* **1976**, 1089.
(43) Compare: Olah, G. A.; Kuhn, S. J. *J. Am. Chem. Soc.* **1964**, *86*, 1067. Myhre, P. C.; Beug, M. *J. Am. Chem. Soc.* **1966**, *88*, 1568 and 1569. Legge, D. I. *J. Am. Chem. Soc.* **1947**, *69*, 2086.
(44) See Schofield in ref 39, p 199 ff and ref 43.

Table VII. Nitration of Polymethylbenzenes with $XPyNO_2^+BF_4^-$ [a]

$XPyNO_2^+BF_4^-$			products (μmol)				
X	μmol	ArH^b (μmol)	$ArNO_2$	$Ar'CH_2NO_2$	Ar'CHX	conv (%)	temp/time (°C/h)
CH_3	45	M (100)	9			19[c]	23/53
H	94	M (220)	28			30	23/3.5
Cl	56	M (120)	55			98[d]	23/1
MeO_2C	63	M (110)	61			97	23/1
NC	84	M (86)	26			31[e]	23/0.3
H	100	D (220)	4.7	22[f]	*g,h*	57	23/29
Cl	36	D (36)	3.4	3.6[f]	*g,j*	86	23/0.1
MeO_2C	40	D (85)	2.3	10.8[f]	*g,k*	88	23/0.1
NC	127	D (156)	4.1	5.9[f]	*g,m*	>32	23/0.1
H	100	P (210)	4.7[n]	11[p]			23/3
Cl	36	P (72)	1.9[n]	6.3[p]			23/0.2
MeO_2C	75	P (152)	9.6[n]	22[p]	*q*	95	23/0.2
NC	100	P (210)	12[n]	4.6[p]	*r*	29	23/0.1
CH_3O	90	H (120)		16	*s*	70	60/24
H	32	H (64)		11	*t*	66	23/12
Cl	36	H (66)		8.9	*u*		23/0.1
MeO_2C	90	H (107)		7.1	*v*	42	23/0.1
NC	84	H (95)		3	*w*	77	23/0.1

[a] In acetonitrile at 23 °C unless indicated otherwise. [b] M = mesitylene, D = durene, P = pentamethylbenzene, H = hexamethylbenzene. [c] $XPyH^+ = 9 \times 10^{-3}$ mmol. [d] $XPyH^+ = 51 \times 10^{-3}$ mmol. [e] $XPyH^+ = 85 \times 10^{-3}$ mmol. [f] 1-NO_2CH_2-2,4,5-$Me_3C_6H_2$. [g] 2,4,5-Trimethylbenzaldehyde (ald), 2,4,5-trimethylbenzyl alcohol (alc), 2,4,5-trimethylbenzyl nitrile (nit), and (2,4,5-trimethylbenzyl)acetamide (amd), and the heptamethyldiphenylmethane dimer (dpm). [h] ald (23) and alc (6.8). [i] No footnote given. [j] ald (5.9), dpm (7.2), and amd (11). [k] alc (3.6), nit (10.8), dpm (0.71), amd (6.9). [l] No footnote given. [m] dpm (9.2), nit (3), amd (21). [n] 2,3,4,5,6-$Me_5C_6NO_2$. [o] No footnote given. [p] 1-NO_2CH_2-2,3,4,5-Me_4C_6H. [q] nit (22), amd (11), and dpm (13). [r] alc (2), amd (6), and dpm (4). [s] amd (22), alc (18), nit (12), $XPyH^+$ (90). [t] nit (10), $XPyH^+$ (33). [u] amd (6), alc (4). [v] amd (2), nit (9), XPy^+ (12). [w] amd (11), alc (7), nit (11), XPy^+ (39), $XPyH^+$ (42). For the footnotes, the quantities in parentheses are in units of micromoles.

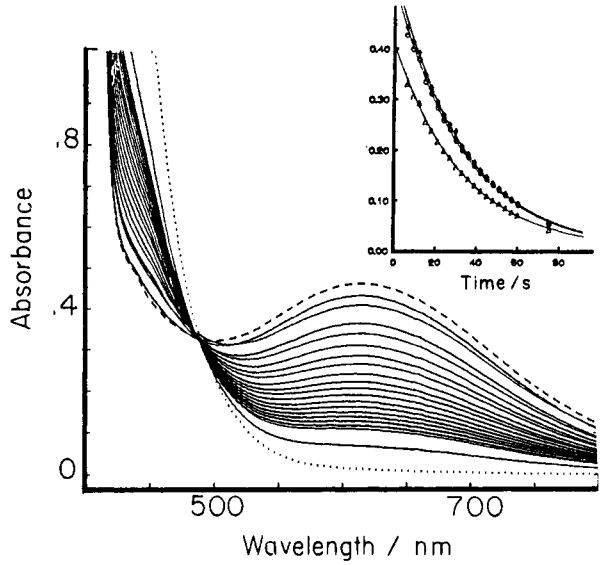

Figure 4. Spontaneous appearance of the charge-transfer absorption band (- - -) upon the mixing of 0.1 M 9-methylanthracene and 0.01 M $MeO_2CPyNO_2^+$ in acetonitrile followed by its decay at 3-s intervals (—) to the final bleached solution (···) at 5 min. The inset shows the calculated fit (—) to first-order kinetics by following the spectral decay at λ 700 (△), 650 (○) and (◆) 600 nm.

ceptors (Table VII). In addition to ring nitration, significant (but variable) amounts of products derived via side chain attack were observed:[45]

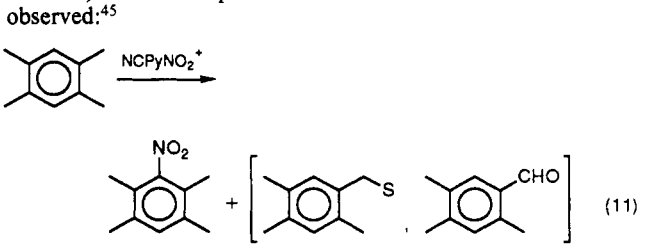

(11)

where S = nitro, nitrito, hydroxy, acetamido, and tetramethylphenyl. The latter were the exclusive products of hexamethylbenzene nitration (entries 14–18). It is also noteworthy that significant amounts of *N*-(pentamethylbenzyl)pyridinium ion were obtained from the treatment of hexamethylbenzene with $NCPyNO_2^+$ (entry 18), less with $MeO_2CPyNO_2^+$ (entry 17), and none with $PyNO_2^+$ (entry 15).

C. Cycloreversion and fragmentation were observed during the nitrations of two selected dimeric aromatic hydrocarbons, viz., the 9-methylanthracene photodimer (MA_2) and 2,3-diphenyl-2,3-butanediol bis(trimethylsilyl) ether (P_2), respectively, with nitropyridinium acceptors. Thus, a dilute solution of MA_2 (0.05 mmol) in dichloromethane upon the addition of an equimolar amount of $MeO_2CPyNO_2^+$ at 25 °C yielded, after 1 h, a complex mixture of nitration products (by GC–MS analysis). The careful separation of the hydrocarbon fraction by thin-layer chromatography afforded 10% (0.005 mmol) 9-methylanthracene (MA) (eq 12).[46]

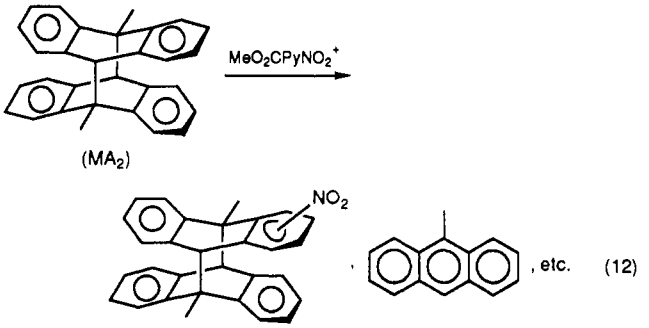

(12)

Since the dianthracene is thermally stable under reaction conditions, we concluded that the monomeric 9-methylanthracene was derived via the cycloreversion of an intermediate produced in the course of nitration.

In an analogous nitration, the pinacol derivative P_2 (0.04 mmol) was treated with an equimolar amount of $MeO_2CPyNO_2^+$ in acetonitrile. The immediate yellow CT coloration was bleached within 5 min, whereupon inspection of the ^1H NMR spectrum

(45) Compare: Blackstock, D. J.; Fischer, A.; Richards, K. E.; Wright, G. J. *Austral. J. Chem.* **1973**, *26*, 775. Suzuki, H.; Koide, H.; Taki, Y.; Ohbayashi, E.; Ogawa, T. *Chem. Lett.* **1987**, 891.

(46) The complex mixture of nitrated products discouraged the establishment of a complete material balance in eq 12.

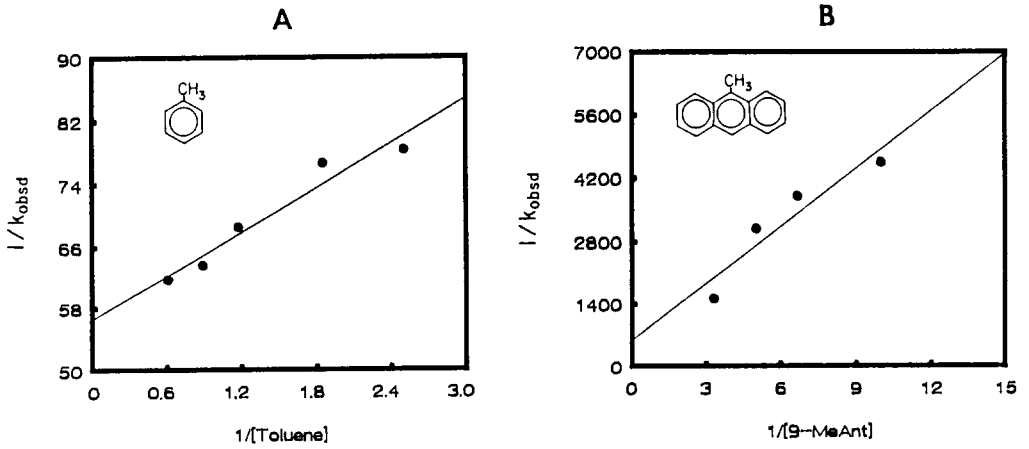

Figure 5. Variation of the nitration rates (k_{obsd}) with the arene concentration according to eq 23 for (A) toluene with $MeO_2CPyNO_2^+$ and (B) 9-methylanthracene with $PyNO_2^+$ in acetonitrile.

revealed the characteristic resonances of acetophenone. Subsequent gas chromatographic and mass spectral analysis after an aqueous workup produced acetophenone in ~10% (0.0043 mmol) yield, together with a complex mixture of nitration products which was not analyzed further.

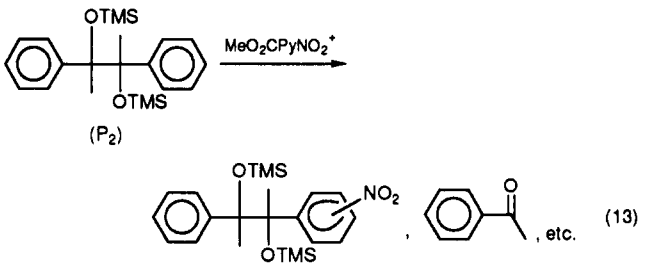

(13)

V. Kinetics of Aromatic Nitration with *N*-Nitropyridinium Acceptors. The varying rates with which the transient colors were bleached from the different *N*-nitropyridinium acceptors were quantitatively evaluated by following the diminution of the associated charge-transfer bands. Thus, the immediate appearance of the well-resolved absorption band with λ_{CT} = 610 nm in Figure 4 corresponded to the spontaneous formation of the EDA complex when $MeO_2CPyNO_2^+$ and 9-methylanthracene were mixed in acetonitrile. The subsequent rapid decay of the charge-transfer band completely back to the baseline within 5 min followed first-order kinetics with the arene in excess. This is shown in the inset of Figure 4 by the fit of the calculated change (smooth lines) in the absorbance (A_{CT} monitored at three selected wavelengths) to the experimental data points, according to the equation:

$$[A_{CT}]_t = [A_{CT}]_0 \exp(-k_{obsd}t)$$

The pseudo-first-order rate constants (k_{obsd}) obtained in this manner with different nitropyridinium acceptors are listed in Table VIII, together with k_{obsd} obtained with different aromatic donors under the same conditions. Most importantly, such a spectrophotometric determination of k_{obsd} for the nitration of mesitylene with $PyNO_2^+$ agreed with the pseudo-first-order rate constant evaluated from product analysis under the same conditions:

$$-dA_{CT}/dt \equiv d[ArNO_2]/dt \qquad (14)$$

where $ArNO_2$ = 1-nitromesitylene. Moreover, the linear dependence of k_{obsd}^{-1} with the systematic variation in the concentrations of two representative aromatic donors (Figure 5) established the overall second-order process

$$-dA_{CT}/dt = k_2[PyNO_2^+][ArH] \qquad (15)$$

where $k_{obsd} = k_2[ArH]_0$.

Substrate selectivity in aromatic nitration was directly measured by the competition method based on the quantitative analysis of the product mixture.[47] The toluene–benzene reactivity ratios k/k_0 in Table IX represent the normalized values derived at 23 °C from $PyNO_2^+BF_4^-$ and $MeO_2CPyNO_2^+BF_4^-$ in combination with various amounts of these aromatic donors in excess to approximate pseudo-first-order conditions. For comparative purposes, the substrate selectivity with $NO_2^+BF_4^-$ was measured at −40 °C to minimize the problems with mixing control.[48] Since the relative reactivities of the other aromatic donors were large, they were evaluated indirectly by the combination of neighboring-pair comparisons, e.g., (mesitylene–toluene and toluene–benzene) = (mesitylene–benzene), etc., as detailed in the Experimental Section.

The kinetic isotope effect for toluene nitration was carried out with $MeO_2CPyNO_2^+$ in acetonitrile using a 20-fold excess of an equimolar mixture of C_7H_8 and C_7D_8 at 23 °C. The value of $k_H/k_D = 0.91 \pm 0.05$ was determined at 12% conversion by the

Table VIII. Spectrometric Rates of Aromatic Nitration with *N*-Nitropyridinium Cations[a]

arene (M)	$XPyNO_2^+BF_4^-$ X	M	λ_{mon}[b] (nm)	k_{obsd} (s^{-1})
benzene (3.40)	MeO_2C	0.20	420–430	2.2×10^{-2}
benzene (0.022)		0.23	360–380[c]	1.3×10^{-2}
toluene (1.65)	MeO_2C	0.020	420–430	1.62×10^{-2}
toluene (1.12)		0.020	420–430	1.57×10^{-2}
toluene (0.86)		0.020	420–440	1.46×10^{-2}
toluene (0.54)		0.020	420–430	1.31×10^{-2}
toluene (0.40)		0.020	420–430	1.28×10^{-2}
p-xylene (0.29)	MeO_2C	0.025	420	1.4×10^{-2}
mesitylene (0.21)	MeO_2C	0.025	420–430	1.2×10^{-2}
mesitylene (0.005)		0.05	410–360	1.1×10^{-2}
1,2,3,5-$(CH_3)_4C_6H_2$ (0.30)		0.025	420–440	2.1×10^{-2}
9-methylanthracene (0.20)	MeO_2C	0.020	600–700	3.6×10^{-2}
9-methylanthracene (0.10)		0.020	600–700	3.0×10^{-2}
toluene (2.67)	H	0.034	420–440	1.4×10^{-5}
mesitylene (0.25)	H	0.025	420–430	6.3×10^{-5}
mesitylene (0.25)		0.025	*d*	5.0×10^{-5}
mesitylene (0.10)		0.010	420, 370–380[c]	3.0×10^{-5}
$(CH_3)_5C_6H$ (0.10)	H	0.010	430–460	2.3×10^{-5}
$(CH_3)_5C_6H$ (0.010)		0.10	450, 390[c]	4.3×10^{-4}
9-methylanthracene (0.30)	H	0.010	580	6.6×10^{-4}
9-methylanthracene (0.20)		0.010	550	3.0×10^{-4}
9-methylanthracene (0.15)		0.010	560	2.5×10^{-4}
9-methylanthracene (0.10)		0.010	520	2.2×10^{-4}
9-methylanthracene (0.010)		0.100	500	1.0×10^{-3}
9-methylanthracene (0.20)	CH_3O	0.020	500–540	1.6×10^{-6}

[a] In acetonitrile at 23 °C. [b] CT band (decrease) monitored, unless indicated otherwise. [c] Appearance of nitration product. [d] Measured by nitromesitylene analysis.

(47) Hoggett, J. G.; Moodie, R. B.; Schofield, K. *J. Chem. Soc. B* **1969**, 1.

(48) Coombes, R. G.; Moodie, R. B.; Schofield, K. *J. Chem. Soc. B* **1968**, 800. Tolgyesi, W. S. *Can. J. Chem.* **1965**, *43*, 343. Christy, P. F.; Ridd, J. H.; Stears, N. D. *J. Chem. Soc. B* **1970**, 797.

Table IX. Competitive Rates of Aromatic Nitration with *N*-Nitropyridinium Cations[a]

				$XPyNO_2^+BF_4^-$		
$(arene)_1$	M_1	$(arene)_2$	M_2	X	M	k_1/k_2
toluene	0.45	benzene	2.1	NC	0.023	48[b]
mesitylene	0.28	anisole	0.60	MeO_2C	0.025	1.4
	0.28	*m*-xylene	0.57		0.025	44
	0.21	toluene	1.0		0.025	89
toluene	0.45	benzene	2.1		0.026	36
	0.47		1.2		0.020	30
	0.41		0.42		0.020	28
	0.90		0.55		0.019	30
	1.79		0.55		0.017	38
	0.41		0.42	Cl	0.04	26
mesitylene	0.21	toluene	1.0	H	0.025	130
	0.27	naphthalene	0.31		0.026	16
	0.28	*m*-xylene	0.57		0.025	6.4
toluene	0.45	benzene	2.13		0.024	32
	0.47		1.15		0.026	31
	0.90		0.55		0.026	32
	1.79		0.55		0.024	41
	0.41		0.42	CH_3	0.034	25
	0.41		0.42	CH_3O	0.045	24[c]
mesitylene	0.19	toluene	0.90	$NO_2^+BF_4^-$	0.014	6.0[b]
	0.21		0.18		0.010	2.9[b]
	0.28		0.11		0.010	3.8[b]
	0.14		0.11		0.010	4.5[b]
toluene	0.14	benzene	0.90		0.012	20[b]
	0.14		0.50		0.014	31[b]
	0.14		0.39		0.012	23[b]
	0.14		0.17		0.014	25[b]
	0.30		0.17		0.012	23[b]
	0.42		0.17		0.012	27[b]

[a] In acetonitrile at 23 °C, unless indicated otherwise. [b] At −42 °C. [c] At 60 °C.

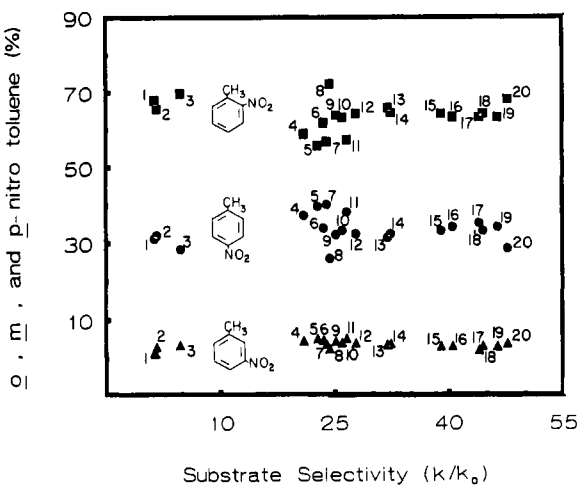

Figure 6. Isomeric composition of nitrotoluenes as a function of the activity of different nitrating agents[49] indicated by their substrate selectivities (k/k_0, toluene relative to benzene).

GC–MS analysis of the mixture of nitrotoluenes (*o*:*m*:*p* = 62:5:32).

Discussion

The *N*-nitropyridinium cations $XPyNO_2^+$ constitute a unique series of nitrating agents in their ability (a) to spontaneously form an extensive family of 1:1 EDA complexes with aromatic donors encompassing various benzene, naphthalene, and anthracene derivatives and (b) to produce a wide array of the corresponding nitration products within the inextensible time span varying from seconds to weeks. Since no other nitrating agent shows both characteristics with an aromatic substrate simultaneously, let us compare the behaviors of $XPyNO_2^+$ and other electrophilic reagents. First, with respect to the distributions of isomeric (nitration) products, the graphic summary in Figure 6 for toluene shows the isomeric composition of *o*-, *m*-, and *p*-nitrotoluenes to be relatively invariant over a very wide range of substrate selectivities (k/k_0 based on the benzene reference) that can be obtained with various nitrating agents.[49-53] Thus, within minor deviations of ±10%, the same distribution of the ortho, meta, and para isomers are formed, irrespective of the reactivity of the nitrating agent. In other words, there is a complete decoupling of the *product-determining step* from the *rate-limiting activation* of aromatic nitration. Such a mechanistic situation would arise when there are two or more reactive intermediates,[54] including the isomeric Wheland or σ-adducts that are common to other nitrating agents[3,39] and the series of nitropyridinium cations pertinent to this study. Second, aromatic nitration with nitropyridinium cations represents one of the few examples in which aromatic substitution is readily effected directly by the active electrophile itself; the other common examples include aromatic metalation, particularly thallation and mercuration, for which the participation of the EDA complexes [ArH, $Tl(O_2CCF_3)_2^+$, and $Hg(O_2CCF_3)_2$, respectively] has been previously delineated.[55] Thus, with respect to EDA complexes in electrophilic aromatic substitution, the linear correlations in Figure 7 underscore the direct relationship of the activation barrier for aromatic nitration with those for aromatic thallation and aromatic mercuration. Such striking linear free energy correlations (with slopes of unity to emphasize the 1:1 relationships) indicate that those factors relevant

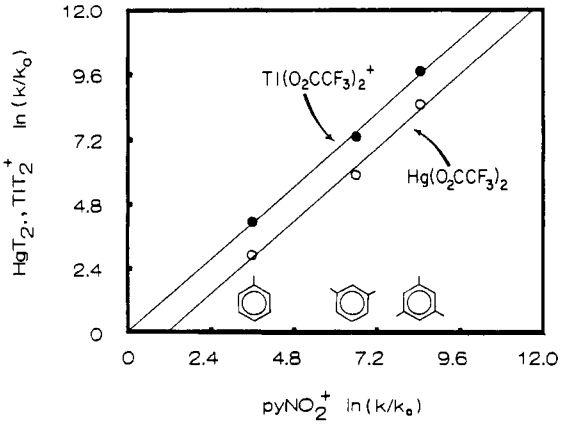

Figure 7. Comparison of the *N*-nitropyridinium acceptor with mercury(II) trifluoroacetate (○) and thallium(III) trifluoroacetate (●) cations in the relative reactivity of toluene, *m*-xylene, and mesitylene in nitration versus mercuration and thallation.

(49) The nitrations listed in Figure 6 are as follows: (1) $NO_2^+PF_6^-$ in $C_4H_8SO_2$ at 25 °C;[12] (2) $NO_2^+BF_4^-$ in $C_4H_8SO_2$ at 25 °C;[12] (3) $NO_2^+BF_4^-$ in CH_3CN at 23 °C;[50] (4) HNO_3 in CH_3NO_2 at 30 °C;[51] (5) ceric ammonium nitrate in CH_3CN at 84 °C;[47] (6) $MeOPyNO_2^+BF_4^-$ in CH_3CN at 60 °C;[50] (7) HNO_3 in HOAc at 45 °C;[52] (8) $NO_2^+BF_4^-$ in CH_3CN at −40 °C;[50] (9) $MePyNO_2^+BF_4^-$ in CH_3CN at 23 °C;[50] (10) $ClPyNO_2^+BF_4^-$ in CH_3CN at 23 °C;[50] (11) $PyNO_2^+$ in CH_3NO_2 at 50 °C;[17b] (12) $MeO_2CPyNO_2^+BF_4^-$ in CH_3CN at 23 °C;[50] (13) same as 12 at −5 °C; (14) $PyNO_2^+BF_4^-$ in CH_3CN at 23 °C;[50] (15) $2,6\text{-}Me_2PyNO_2^+BF_4^-$ in CH_3CN at ~25 °C;[17b] (16) $2,4\text{-}Me_2PyNO_2^+BF_4^-$ in CH_3CN at ~25 °C;[17b] (17) $CH_3CO_2NO_2$ in CH_3CN;[53] (18) $2,6\text{-}Me_2\text{-}4\text{-}MeOPyNO_2^+BF_4^-$ in CH_3CN at ~25 °C;[17b] (19) 2-Me-4-$MeOPyNO_2^+BF_4^-$ in CH_3CN at ~25 °C;[17b] and (20) $NCPyNO_2^+BF_4^-$ in CH_3CN at −40 °C.[50] Note that the substrate selectivities for NO_2^+ salts as given in Figure 6 are based on the raw data and thus subject to mixing control.[48]

(50) See the Experimental Section.

(51) Ingold, C. K.; Lapworth, A.; Rothstein, E.; Ward, D. *J. Chem. Soc.* **1931**, 1959.

(52) Cohn, H.; Hughes, E. D.; Jones, M. H.; Peeling, M. G. *Nature* **1952**, *169*, 291.

(53) Olah, G. A. *Acc. Chem. Res.* **1971**, *4*, 240.

(54) For a detailed discussion of this important point, see: Olah, G. A. et al. in ref 3, p 134 ff and Olah, G. A.; Narang, S. C.; Olah, J. A. *Proc. Natl. Acad. Sci. USA* **1981**, *78*, 3298. However, note that the ground-state EDA complex, which is equivalent to Olah's π-complex, is not to be included among the reactive intermediates (see Table II). Furthermore, the very rapid (thermodynamic) equilibration among the isomeric Wheland intermediates, which could lead to the constant isomer distribution in Figure 6, is disfavored by the absence of a base or medium effect on deprotonation (compare also Table 41 in ref 3).

(55) Lau, W.; Kochi, J. K. *J. Am. Chem. Soc.* **1986**, *108*, 6720; **1984**, *106*, 7100.

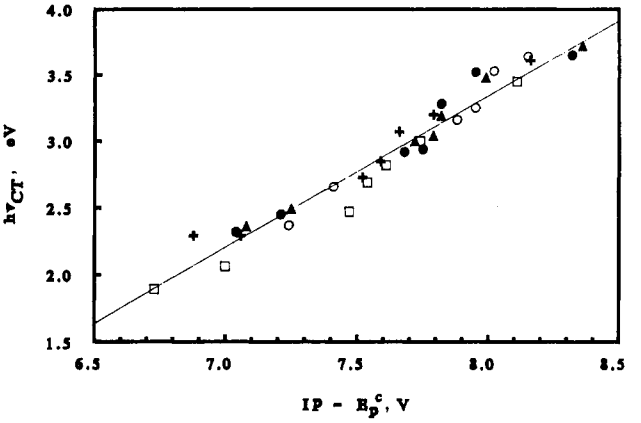

Figure 8. Mulliken correlation of the charge-transfer transition energies ($h\nu_{CT}$) with the HOMO–LUMO gap for the aromatic EDA complexes with $XPyNO_2^+$ listed in Tables I and III.

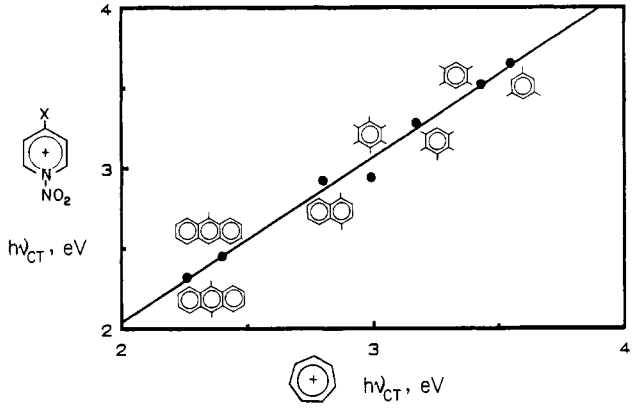

Figure 9. Direct relationship of *N*-nitropyridinium and tropylium acceptors as measured by the charge-transfer transition energies in various aromatic EDA complexes.

to surmounting the activation barriers are equivalent—despite the marked difference in the stoichiometry for aromatic nitration,

$$ArH + PyNO_2^+ \rightarrow ArNO_2 + PyH^+ \quad (16)$$

aromatic thallation,

$$ArH + Tl(O_2CCF_3)_2^+ \rightarrow ArTl(O_2CCF_3)_2 + H^+ \quad (17)$$

and aromatic mercuration.

$$ArH + Hg(O_2CCF_3)_2 \rightarrow ArHgO_2CCF_3 + CF_3CO_2H \quad (18)$$

Accordingly, the search for a unifying theme turns our attention to the EDA complex, as follows.

I. Charge-Transfer Structures of Aromatic EDA Complexes with $XPyNO_2^+$. The various *N*-nitropyridinium cations are excellent electron acceptors by virtue of the wide range of charge-transfer ($h\nu_{CT}$) interactions that are induced with different aromatic donors, as shown by the family of characteristic intermolecular absorption bands in Figure 1. The acceptor properties of nitropyridinium are quantitatively evaluated by a reduction potential E_p^c (Table III), which spans a range of ~15 kcal mol^{-1} simply by the replacement of a *p*-methoxy substituent in the pyridine moiety by a cyano group. As a result, the charge-transfer energies for the series of aromatic EDA complexes in Table I vary by almost 50 kcal mol^{-1}. The linear correlation shown in Figure 8 can be analytically expressed by the Mulliken correlation as eq 19:

$$h\nu_{CT} = IP - E_p^c - 4.71 \quad (19)$$

where the energy gap $IP - E_p^c$ represents the HOMO–LUMO separation of the aromatic donor and the nitropyridinium acceptor in the EDA complex.[30] The slope of unity in Figure 8 reflects the formation of a series of uniformly weak EDA complexes,[9,30] and it is supported by the spectrophotometric measurements in Table II. Furthermore, the spectral properties of these EDA complexes are strongly correlated in Figure 9 with those extant in the corresponding aromatic complexes with the tropylium cation:[56]

$$h\nu_{CT}(XPyNO_2^+) = h\nu_{CT}(C_7H_7^+) - 0.02 \quad (20)$$

with $r = 0.994$. Since the latter are known to exist as 1:1 π-complexes,[57] it is reasonable to propose an analogous cofacial structure for the nitropyridinium complexes, as graphically depicted below.[58] It is important to emphasize that the limited

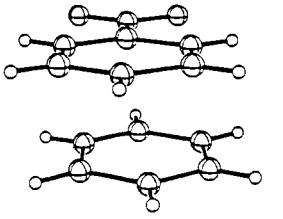

values for K_{EDA} of roughly 1 in Table II indicate the formation of all the EDA complexes to be essentially thermoneutral (i.e., $\Delta G_{EDA} \approx 0$), irrespective of the anthracene, naphthalene, and benzene donor employed and for every nitropyridinium acceptor. As such, the transient appearance of [ArH,X-$PyNO_2^+$] in the course of aromatic nitration must be considered only as a rapid equilibrium step,[59] with no profound ramifications on the activation process(es).

II. Aromatic Nitration via the EDA Complexes with $XPyNO_2^+$. The broad range of charge-transfer energies ($h\nu_{CT}$) of the aromatic EDA complexes with $XPyNO_2^+$ parallel an equally broad range of thermal reactivities. Indeed the nitropyridinium salts form a steeply graded series of nitrating agents, since at one extreme the *p*-cyano and *p*-carbomethoxy derivatives $NCPyNO_2^+$ and $MeO_2CPyNO_2^+$ (practically) rival the most reactive nitrating agents such as nitronium tetrafluoroborate,[60] nitric acid with sulfuric acid,[61] etc., and at the other extreme the *p*-methoxy derivative $MeOPyNO_2^+$ is almost as inert as methyl nitrate (in the absence of an acid catalyst).[3] Thus benzene, naphthalene, and anthracene donors all react at room temperature with the highly electron-deficient acceptor $MeO_2CPyNO_2^+$ within a time span of minutes to seconds, but the more electron-rich acceptor $MeOPyNO_2^+$ requires more than a week to react with an anthracene donor under the same conditions. The expressions in eqs 14 and 15 emphasize the direct relationship between the second-order kinetics for the decay of the CT absorption band and the appearance of nitration products. Coupled with the limited magnitudes of the formation constants for the EDA complexes (Table II), the rate data are in accord with the following pathway for the direct involvement of the nitropyridinium acceptor in aromatic nitration.[62]

Scheme I

$$ArH + XPyNO_2^+ \overset{K_{EDA}}{\rightleftharpoons} [ArH,XPyNO_2^+] \quad (21)$$

$$[ArH,XPyNO_2^+] \xrightarrow{k_1} ArNO_2 + XPyH^+ \quad (22)$$

According to Scheme I, the 1:1 EDA complex is formed in low steady-state concentration in the rapid preequilibrium step (eq 21),[59] and it subsequently disappears by the slow rate-determining

(56) Feldman, M.; Winstein, S. *J. Am. Chem. Soc.* **1961**, *83*, 3338. Dauben, H. J., Jr.; Wilson, J. D. *J. Chem. Soc., Chem. Commun.* **1968**, 1629.
(57) Takahashi, Y.; Sankararaman, S.; Kochi, J. K. *J. Am. Chem. Soc.* **1989**, *111*, 2954.
(58) Drawn to scale according to Takahashi et al. in ref 57. See also: Prout, C. K.; Kamenar, B. In *Molecular Complexes*; Foster, R., Ed.; Elek Science: London, 1973; Vol. 1, p 151 ff.
(59) The rates of formation of such EDA complexes are diffusion controlled.[6,7]
(60) Kuhn, S. J.; Olah, G. A. *J. Am. Chem. Soc.* **1961**, *83*, 4564.
(61) Seidenfaden, W.; Pawellek, D. In *Methoden der Organischen Chemie*; Houben-Weyl, Thieme: Stuttgart, 1971; Vol. 12, p 475 ff.
(62) Note that the overall second-order kinetics in eq 15 is consistent with the formulation in Scheme I where K_{EDA} is of limited magnitude (Table II).

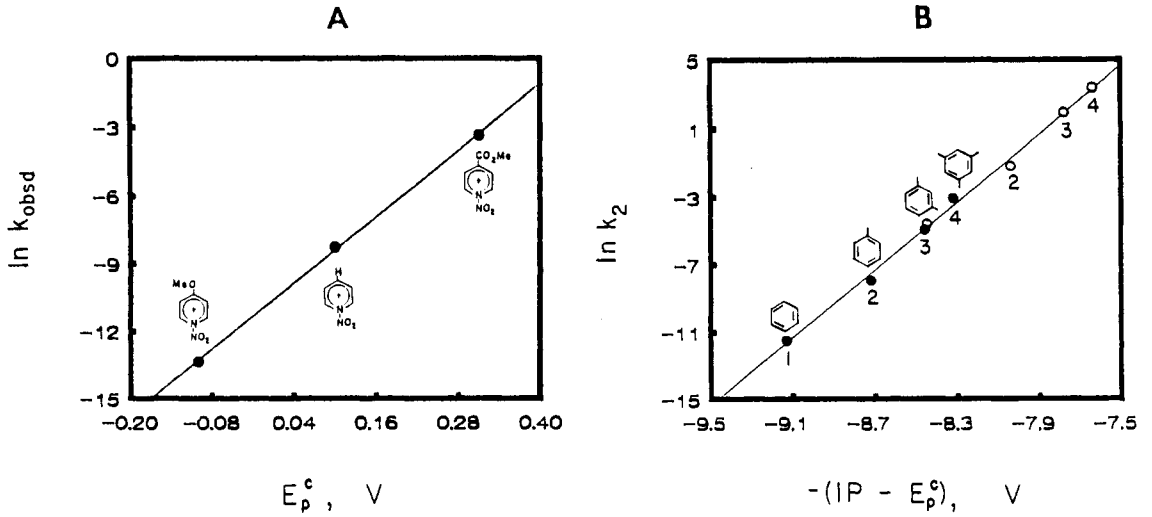

Figure 10. Structural effects of the driving force as given by (A) the E_p^c values of $XPyNO_2^+$ relative to the reactivity (ln k_{obsd}) toward 9-methylanthracene and (B) the HOMO–LUMO gap between $PyNO_2^+$ (●) or $MeO_2CPyNO_2^+$ (○) and the aromatic donors indicated relative to their nitration rates.

step in eq 22.[63] If so, the pseudo-first-order rate constant in Table VIII is given as eq 23:

$$k_{obsd}^{-1} = k_1^{-1} + k_1 K_{EDA}[ArH]_0^{-1} \quad (23)$$

where $[ArH]_0$ represents the aromatic donor in excess. Indeed, the formation constant $K_{EDA} = 1.4\ M^{-1}$ obtained from the plot in Figure 5B for methylanthracene and $PyNO_2^+$ agrees with the value of K_{EDA} evaluated directly by the spectrophotometric procedure of Benesi and Hildebrand[29] (see Table II, entry 2). Most importantly, the applicability of eq 23 shows that an alternative mechanism based on the slow rate-limiting dissociation of the nitropyridinium acceptor

Scheme II

$$XPyNO_2^+ \xrightarrow{k_1} XPy + NO_2^+ \quad (24)$$

$$NO_2^+ + ArH \rightarrow Ar(H)NO_2^+ \quad (25)$$

is not a kinetically viable pathway, since aromatic nitration with the nitronium ion in the followup step (eq 25) is encounter controlled,[48,65] and the ultimate deprotonation of the Wheland intermediate is not rate-limiting.[66] As such, the mechanism in Scheme I coincides with the idea of *transfer nitration* originally conceived by Olah and co-workers.[17a] However, it leaves open the critical question as to how the nitro group is actually transferred from the (coordinatively saturated) nitropyridinium acceptor to the aromatic donor to form the Wheland intermediate in eq 1.[67] Accordingly, let us consider the activation process for aromatic nitration from both the reactivity of the nitropyridinium acceptor as well as that of the aromatic donor.

III. Charge-Transfer Activation of Aromatic EDA Complexes with $XPyNO_2^+$. The strong rate dependence on the acceptor strength is illustrated in Figure 10A,[68] which underscores the direct influence of the 1-electron reduction potential on the activation barrier for $XPyNO_2^+$ reactivity. Similarly, the reactivity of the aromatic substrates in Table IX parallels their donor strengths as given by the (negative) ionization potentials, i.e., −IP, in the following order: benzene < toluene < *m*-xylene < mesitylene.[27] The combined effect of the various donors and nitropyridinium acceptors is considered in Figure 10B[69] from the perspective of the HOMO–LUMO gap in the EDA complex. Since the latter is described by eq 19, the linear correlation in Figure 10B is tantamount to an activation barrier for aromatic nitration, which is strongly affected by the energy ($h\nu_{CT}$) of the charge-transfer excited state:[7]

$$[ArH,X\text{-}PyNO_2^+] \xrightarrow{h\nu_{CT}} [ArH^{\bullet+},XPyNO_2^{\bullet}] \quad (26)$$

The HOMO–LUMO gap is also intrinsic to the theoretical models for nucleophile/electrophile reactivity based on either the charge and frontier orbital control of Klopman[71] or the curve-crossing diagrams for mixing electronic configurations of Shaik and Pross.[72] The visualization of these theoretical constructs for nitro transfer can be facilitated by considering the nitration mechanism in several discrete steps.

Scheme III

$$[ArH,XPyNO_2^+] \underset{k_{-1}}{\overset{k_1}{\rightleftharpoons}} [ArH^{\bullet+},XPyNO_2^{\bullet}] \quad (27)$$

$$[ArH^{\bullet+},XPyNO_2^{\bullet}] \xrightarrow{fast} [ArH^{\bullet+},NO_2,XPy] \quad (28)$$

$$[ArH^{\bullet+},NO_2,XPy] \rightarrow Ar\overset{+}{\underset{NO_2}{\overset{H}{<}}} + XPy \quad (29)$$

The activation process in eq 27 represents the thermal (adiabatic) counterpart to the charge-transfer excitation of the EDA complex in eq 26.[73] The subsequent, spontaneous fragmentation of the nitropyridinyl radical in eq 28 follows from the transient electrochemical studies of $XPyNO_2^+$ (see eq 8).[35] Finally, the formation of the Wheland intermediate via the collapse of the ion radical pair in eq 29 is supported by recent time-resolved spectroscopic studies of $[ArH^{\bullet+},NO_2]$.[74]

(63) The alternative formulation should be mentioned here, since it is commonly asked whether the EDA complex is a precursor (as in Scheme I) or involved in an unproductive, side equilibrium. Although the two pathways are kinetically indistinguishable, the actual distinction is dubious and possibly even meaningless.[64]

(64) See: Colter, A. K.; Dack, M. R. J. In *Molecular Complexes*; Foster, R., Ed.; Crane, Russak: New York, 1974; Vol. 2, p 2 ff. Also see: footnote 20 in Fukuzumi, S.; Kochi, J. K. *J. Am. Chem. Soc.* **1980**, *102*, 2141.

(65) Rys, P. *Angew. Chem., Int. Ed. Engl.* **1977**, *16*, 807.

(66) Melander, L.; Saunders, W. H., Jr. In *Reaction Rates of Isotopic Molecules*; Wiley: New York, 1980; p 162 ff.

(67) For example, the concerted displacement of pyridine from $PyNO_2^+$ by most aromatic donors appears to be unfavored relative to the microscopic reverse process.

(68) Based on the data in Table VIII for methylanthracene, the linear relationship in $RT \ln k_{obsd} = 0.6\ E_p^c - 0.3$ when the energy units are expressed in volts.

(69) The reactivity (log *k*) of an aromatic donor relative to the benzene reference is calculated from the data in Table IX (see the Experimental Section for details). The linear expression is $RT \ln k = -0.3\ (IP - E_p^c) + 2.21$, expressed in volts.

(70) See: Kochi, J. K. *Acta Chem. Scand.* **1990**, *44*, 409.

(71) Klopman, G. *J. Am. Chem. Soc.* **1968**, *90*, 223. Klopman, G. In *Chemical Reactivity and Reaction Paths*; Wiley: New York, 1974; p 55 ff.

(72) Shaik, S. S. *Pure Appl. Chem.* **1991**, *63*, 195; *Acta Chem. Scand.* **1990**, *44*, 205. Pross, A. *Adv. Phys. Org. Chem.* **1985**, *21*, 99; *Acc. Chem. Res.* **1985**, *18*, 212. Shaik, S. S.; Pross, A. *J. Am. Chem. Soc.* **1989**, *111*, 4306.

(73) Since the electron transfer in eq 26 is likely to proceed via an inner-sphere mechanism, Marcus theory cannot be applied indiscriminately. For a discussion of this important point, see: Kochi, J. K. *Angew. Chem., Int. Ed. Engl.* **1988**, *27*, 1227; *Acc. Chem. Res.*, submitted for publication. Compare also: Eberson, L.; Radner, F. *Acc. Chem. Res.* **1987**, *20*, 53.

According to the charge-transfer formulation in Scheme III, the substrate selectivity for aromatic nitration is largely controlled by the activation process in eq 27, whereas the isomeric product distribution is separately established in a subsequent step (eq 29).[75] The guidelines for ascertaining the reactivity and accounting for the products from different nitropyridinium cations can be summarized as follows.

A. Reactivity. Since the driving force for charge-transfer activation of the EDA complex depends on the HOMO–LUMO gap, the rates of aromatic nitration will increase with the values of E_p^c for $XPyNO_2^+$ in the following order: X = CN ≫ CO_2CH_3 > Cl > H > CH_3 ≫ OCH_3 (see Table III). If the sequence in Scheme III is also applied to other nitronium carriers YNO_2, such as nitric acid, acetyl nitrate, tetranitromethane, etc., the activation process will be more generally represented by the combination of eqs 27 and 28 owing to differences in $YNO_2^{\bullet}$ lifetimes.[77] In the extreme case of the highly reactive, coordinatively unsaturated NO_2^+ acceptor, the direct formation of the relevant ion radical pair [$ArH^{\bullet+}$,NO_2] is possible.[78] The observation of a small secondary deuterium kinetic isotope effect (k_H/k_D = 0.85, 0.89)[12] for the nitration of toluene and benzene with $NO_2^+BF_4^-$ is consistent with charge-transfer activation.[76] The presence of the pyridine base has no effect on the kinetics since k_H/k_D = 0.91 for toluene nitration with $MeO_2CPyNO_2^+$.

B. Isomeric Product Distribution. The step in Scheme III (eq 29) that leads to the critical Wheland intermediate does not depend on the nucleofugal group Y of the nitrating agent (YNO_2). It follows that the isomeric product distribution in aromatic nitration will be independent of the nitrating agent, including $NO_2^+BF_4^-$ itself. Indeed the results illustrated in Figure 6 show that essentially the same mixture of *o*-, *m*-, and *p*-nitrotoluenes are obtained from nitrations carried out with (a) $MeOPyNO_2^+$ at 50 °C, (b) $MeO_2CPyNO_2^+$ at 23 °C, (c) $NCPyNO_2^+$ at −17 °C, and (d) NO_2^+ at −40 and 23 °C to represent the sharply increasing order in the reactivity of the nitrating agent. It is also important to emphasize that the pyridine (XPy) that is liberated from these nitrating agents in eq 28 has no or little effect on the isomeric product distribution, although it can cover a wide span of base strength (e.g., ΔpK = 4.7 from MeOPy to NCPy).[38] Moreover, the same conclusion can be reached from the extensive data set (with more than 100 reagent combinations) compiled by Olah, Malhotra, and Narang[3] for toluene nitration carried out in either highly acidic, neutral, protic, or nonpolar media with structurally diverse nitrating agents from −78 to beyond 100 °C![79]

IV. Nonconventional Byproducts from Aromatic Nitrations with $XPyNO_2^+$. As important as the charge-transfer contribution may be in aromatic nitration, the experimental basis for establishing whether the ion radical pair [$ArH^{\bullet+}$,NO_2] is or is not an actual intermediate is difficult to prove. Thus in the thermal (adiabatic) process, the concentration of a reactive intermediate such as the ion radical pair will be too low to detect directly, since its annihilation will perforce be faster than its rate of production. However, there is ample indirect evidence based on nonconventional byproducts[80] that reactive intermediates can be partitioned during aromatic nitration. Thus, the extensive transfer of the *tert*-butyl substituent in the nitration of *tert*-butylbenzene (Table V) and 1,4-di-*tert*-butylbenzene (Table VI) is symptomatic of an ipso (Wheland) adduct:[81]

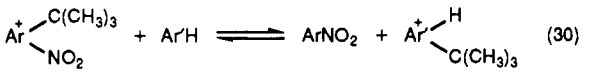

(30)

Similarly, the extensive side chain substitution of durene in eq 11 (together with pentamethylbenzene and hexamethylbenzene in Table VII) can proceed via a methylenecyclohexadiene intermediate followed by sigmatropic rearrangement:[82]

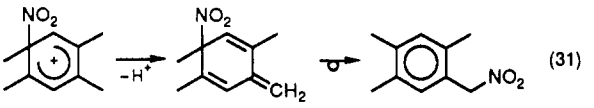

(31)

However, there is an alternative charge-transfer pathway proceeding through the durene ion radical pair which is known to be readily deprotonated and lead to side chain substitution.[83]

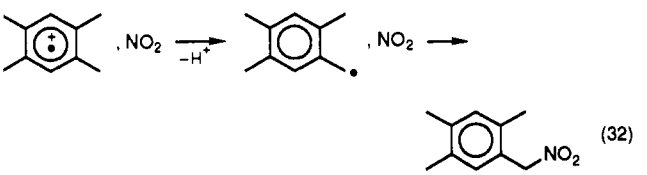

(32)

The evidence for the aromatic cation radical is more direct in the partial cycloreversion of the dianthracene MA_2 as a result of its exposure to $MeO_2CPyNO_2^+$ in eq 12. Although the dianthracene is thermally robust, the cation radical is known to undergo a rapid fragmentation with the first-order rate constant of $k'_1 \approx 10^8\ s^{-1}$.[84]

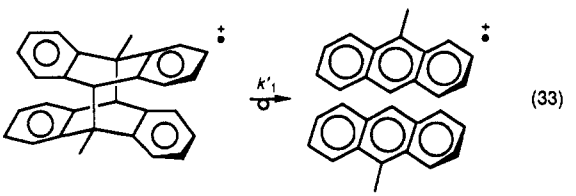

(33)

Such a significant cycloreversion of the dianthracene is readily accommodated by the competition in Scheme III, with the rate constant for back electron transfer estimated to be $k_{-1} \approx 10^9\ s^{-1}$ in eq 27.[85] Similarly, the retro-pinacol of P_2 to yield acetophenone during its treatment with $MeO_2CPyNO_2^+$ in eq 13 is consistent with the very short lifetime ($\tau \approx 2 \times 10^{-10}$ s) that has been established for the aromatic cation radical ($P_2^{\bullet+}$),[86] where X =

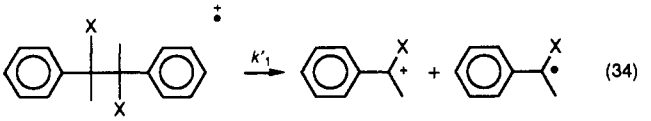

(34)

$OSi(CH_3)_3$. Moreover, the nitration of bicumene by $MeO_2CPyNO_2^+$ with no or little accompanying fragmentation (see the Experimental Section) accords with the significantly

(74) Sankararaman, S.; Haney, W. A.; Kochi, J. K. *J. Am. Chem. Soc.* **1987**, *109*, 5235 and 7824. Bockman, T. M. Unpublished results.

(75) For the regiospecificity in the collapse of the ion radical pair to the isomeric Wheland intermediates, see ref 76, Petersen, Perrin, et al. in ref 13, and Epiotis, N. D. *J. Am. Chem. Soc.* **1973**, *95*, 3188.

(76) Fukuzumi, S.; Kochi, J. K. *J. Am. Chem. Soc.* **1981**, *103*, 7240.

(77) As an example, the electrochemical EC process is driven by the chemical followup step; see: Bard and Faulkner in ref 37a, p 454 ff.

(78) For the relevant reduction potential of NO_2^+ and the inner-sphere pathway for electron transfer, see: Lee, K. Y.; Amatore, C.; Kochi, J. K. in ref 36a. For the electronic structure and kinetic behavior of [$ArH^{\bullet+}$, NO_2], compare with the recent studies of the nitric oxide analogue described in ref 87 and by Bockman, T. M.; Karpinski, Z. J.; Kochi, J. K. *J. Am. Chem. Soc.*, in press.

(79) The isomeric compositions in Table 41 of ref 3 are strikingly invariant within ±10% for *o*- and *p*-nitrotoluene. We previously emphasized,[21] and Figure 6 graphically illustrates, the importance of product compositions (and not product ratios) as the informative measure of the competitive formation of isomers.

(80) Hartshorn, S. R. *Chem. Soc. Rev.* **1974**, *3*, 167. Suzuki, H. *Synthesis* **1977**, 217.

(81) Perrin, C. L.; Skinner, G. A. *J. Am. Chem. Soc.* **1971**, *93*, 3389. Perrin, C. L. *J. Org. Chem.* **1971**, *36*, 420. Myhre, P. C. *J. Am. Chem. Soc.* **1972**, *94*, 7921. Fischer, A.; Ramsay, J. N. *J. Chem. Soc., Perkin Trans. 2* **1973**, 237; *J. Am. Chem. Soc.* **1974**, *96*, 1614.

(82) Fischer, A.; Goel, A. *J. Chem. Soc., Chem. Commun.* **1988**, 526.

(83) Masnovi, J. M.; Sankararaman, S.; Kochi, J. K. *J. Am. Chem. Soc.* **1989**, *111*, 2263.

(84) Masnovi, J. M.; Kochi, J. K. *J. Am. Chem. Soc.* **1985**, *107*, 6781.

(85) By taking an ~10% yield of methylanthracene. It is also possible for cycloreversion to occur by ipso addition, followed by the heterolytic scission of the 9,9′ bond.

(86) Sankararaman, S.; Perrier, S.; Kochi, J. K. *J. Am. Chem. Soc.* **1989**, *111*, 6448. Retro-pinacol by ipso addition, as outlined in footnote 85, is less likely for P_2 owing to the highly hindered (neopentyl-like) position.

longer lifetime of bicumene cation radical.[86] It is also noteworthy that both the dianthracene MA_2 and the pinacol P_2 react with $MeO_2CPyNO_2^+$ much faster than expected relative to the nitration rates of *o*-xylene and *tert*-butylbenzene, respectively, taken as the simple reference donors. Such a rate acceleration is commonly observed in the charge transfer of an aromatic donor that is driven by the rapid fragmentation of $ArH^{\bullet+}$ applicable to Scheme III,[87] but it is not easily explained by eq 1 involving a direct (ipso) attack.[88] Thus, to account for all of the experimental facts, we believe that the dissection of the aromatic nitration rate into discrete steps (as represented in Scheme III) provides a mechanistically useful paradigm that is not so obviously provided by theoretical constructs.[71,72]

Summary and Conclusions

The spontaneous formation of charge-transfer complexes occurs upon the mixing of various benzenes, naphthalenes, and anthracenes (ArH) with a series of nitropyridinium cations $XPyNO_2^+$. The ensuing aromatic nitrations are effected over a wide range of rates that track the HOMO–LUMO gap of the [ArH,$XPyNO_2^+$] complexes. The charge-transfer activation for aromatic nitration as presented in eq 27 (Scheme III) provides the common theme for unifying aromatic nitration with other electrophilic aromatic substitutions, such as thallation and mercuration in eqs 17 and 18. Especially pertinent is the need to consider the followup process as presented in eq 28 for the fragmentation of $XPyNO_2^{\bullet}$ during nitration (and of $Hg(O_2CCF_3)_2^{\bullet-}$ during mercuration) in evaluating the overall driving force for charge transfer.[88] When such an activation of the charge-transfer process is cleanly delineated, the isomeric product distribution for aromatic substitution will show no (or little) dependence on the structure of the electrophilic reagent.

Experimental Section

Materials. Benzene (Baker), toluene (Baker), *p*-xylene (Eastman), *m*-xylene (Aldrich), isodurene (Aldrich), and mesitylene (Aldrich) were distilled from sodium. Durene (Aldrich), pentamethylbenzene (Aldrich), hexamethylbenzene (Aldrich), and 9-methylanthracene (Aldrich) were recrystallized from absolute ethanol. Chlorobenzene (Aldrich), bromobenzene (Aldrich), iodobenzene (Aldrich), and *tert*-butylbenzene (Aldrich) were distilled, and naphthalene (Aldrich) was sublimed. 1,4-Dimethylnaphthalene (Aldrich), 9,10-dimethylanthracene (Aldrich), hexamethyl(Dewar benzene) (Aldrich), 1,3-di-*tert*-butylbenzene (Aldrich), and 1,4-di-*tert*-butylbenzene (Aldrich) were used as received. The isomeric purity of each aromatic hydrocarbon was established by gas chromatographic analysis. The dianthracene derivative MA_2 was synthesized via the photodimerization of 9-methylanthracene in dichloromethane by irradiation at 350 nm in a Rayonet photochemical reactor.[89] The pinacol derivative P_2 was synthesized according to a literature procedure.[86] Acetonitrile (Fisher) was stirred with $KMnO_4$ for 24 h, and the mixture was refluxed until the liquid was colorless. After removal of the brown MnO_2 by filtration, the acetonitrile was distilled from P_2O_5 under an argon atmosphere. Acetonitrile was again fractionated from CaH_2 and stored in a Schlenk flask under an argon atmosphere. For the reactions of $NO_2^+BF_4^-$, acetonitrile was passed through dried neutral alumina (baked at 350 °C at 0.01 mmHg for 20 h) under an argon atmosphere prior to use. Chloroform was washed with water, dried over K_2CO_3, and then fractionated from P_2O_5 under an argon atmosphere and stored in a Schlenk flask in the dark. Ethyl ether was refluxed and distilled from $LiAlH_4$. Nitromethane was crystallized at −78 °C and then passed through dried neutral alumina under an argon atmosphere. The nitromethane was fractionated under reduced pressure (150 mmHg) and stored in a Schlenk flask in the dark. Nitric acid was obtained from the distillation of a mixture of 90% nitric acid (250 mL), concentrated sulfuric acid (250 mL), and 2.5 g of urea at ambient temperatures under reduced pressure. Anhydrous nitric acid was collected in a dry ice trap and stored as a colorless liquid at −20 °C. $NO_2^+BF_4^-$ was prepared from anhydrous nitric acid, anhydrous HF, and BF_3 in dichloromethane following Elsenbaumer's procedure.[22] Recrystallization of the crude product from a mixture of acetonitrile and dichloromethane at −40 °C yielded colorless crystals of $NO_2^+BF_4^-$.[78] The purity of $NO_2^+BF_4^-$ was assayed (>98%) by GC and NMR analysis of 2,4-dinitrotoluene from the treatment of *p*-nitrotoluene in CD_3CN. The IR spectrum of the 18-crown-6 complex with $NO_2^+BF_4^-$ in dichloromethane showed no absorption bands due to the nitrosonium impurity. 4-Picoline (Aldrich) was purified via the hydrochloride, and then it was distilled from solid KOH. Pyridine (Mallinckrodt) was distilled from KOH. 4-Methoxypyridine was prepared by hydrogenation of 4-methoxypyridine *N*-oxide (Aldrich) with 10% Pd/C in ethanol followed by distillation. 4-Chloropyridine was prepared by neutralization of the 4-chloropyridine hydrochloride salt (Aldrich) with aqueous KOH, followed by distillation from solid KOH. Methyl isonicotinate (Aldrich) was distilled prior to use, and 4-cyanopyridine (Aldrich) was recrystallized from ethanol.

Crystalline 4-$XPyNO_2^+BF_4^-$ salts were prepared from pure $NO_2^+BF_4^-$ and the appropriate pyridine to avoid contamination by a nitrosonium impurity as follows.

A. $PyNO_2^+BF_4^-$ was prepared from $NO_2^+BF_4^-$ and 1 equiv of pyridine at 0 °C following Olah's procedure.[17] Recrystallization from a mixture of acetonitrile and chloroform at −20 °C afforded colorless crystals of $PyNO_2^+BF_4^-$: ^1H NMR (CD_3CN) δ 9.71 (d, 2 H, J = 7.2 Hz), 8.99 (t, 1 H, J = 7.7 Hz), 8.35 (t, 2 H, J = 7.7 Hz); IR (CH_3CN) 3119, 1721, 1605, 1284, 1100–1000, 812, 721, 654 cm^{-1}.

B. 4-$MePyNO_2^+BF_4^-$ was obtained from $NO_2^+BF_4^-$ and 4-picoline in CH_3CN at −20 °C. Recrystallization from a mixture of acetonitrile and ethyl ether at −20 °C yielded the colorless crystalline salt: ^1H NMR (CD_3CN) δ 9.51 (d, 2 H, J = 7.5 Hz), 8.11 (d, 2 H), 2.82 (s, 3 H); IR (CH_3CN) 3119, 1714, 1617, 1290, 1100–1000, 836, 794 cm^{-1}.

C. 4-$MeOPyNO_2^+BF_4^-$. To a cold suspension of 1.2 g of $NO_2^+BF_4^-$ in 150 mL of acetonitrile was slowly (1 h) added a solution of 0.9 mL of 4-methoxypyridine dissolved in 50 mL of acetonitrile at −20 °C. After the addition, stirring was continued for an additional hour at −20 °C. The solvent was removed in vacuo. The pale yellow residue was crystallized from a mixture of acetonitrile and ethyl ether at −20 °C: ^1H NMR (CD_3CN) δ 9.46 (dd, 2 H, J = 6.1, 2.0 Hz), 7.55 (dd, 2 H), 4.29 (s, 3 H); IR (CH_3CN) 3131, 1696, 1623, 1514, 1272, 1100–1000, 848, 794, 557, 521 cm^{-1}. Anal. Calcd for $C_6H_7BF_4N_2O_3$ (242.0): C, 29.78; H, 2.92; N, 11.58. Found: C, 29.66; H, 2.90; N, 11.08.

D. 4-$ClPyNO_2^+BF_4^-$. The reaction was carried with 4-chloropyridine at 0 °C following the procedure used for $MeOPyNO_2^+BF_4^-$. The colorless crystalline salt was obtained by recrystallization from a mixture of acetonitrile and chloroform at −20 °C. This salt was highly moisture-sensitive and immediately turned orange upon exposure to the air: ^1H NMR (CD_3CN) δ 9.63 (d, 2 H, J = 7.6 Hz), 8.33 (d, 2 H); IR (CH_3CN) 3119, 1726, 1623, 1278, 1266, 1100–1000, 812, 727, 521 cm^{-1}.

E. 4-$CH_3O_2CPyNO_2^+BF_4^-$. This very moisture-sensitive salt was synthesized from methyl isonicotinate and purified following the same procedure as for 4-$ClPyNO_2^+BF_4^-$: ^1H NMR (CD_3CN) δ 9.84 (d, 2 H, J = 7.4 Hz), 8.69 (d, 2 H), 4.05 (s, 3 H); IR (CH_3CN) 3119, 1747, 1731, 1622, 1288, 1100–1000, 798, 720, 668 cm^{-1}.

F. 4-$NCPyNO_2^+BF_4^-$. The synthesis and purification of this highly sensitive salt were carried out with 4-cyanopyridine following the same procedure as for 4-$ClPyNO_2^+BF_4^-$: ^1H NMR (CD_3CN) δ 9.89 (d, 2 H, J = 7.4 Hz), 8.68 (d, 2 H); IR (CH_3CN) 3113, 1738, 1617, 1284, 1100–1000, 854, 818, 775, 733, 533 cm^{-1}.

G. $PyNO_2^+SbCl_6^-$. $NO_2^+SbCl_6^-$ was prepared from NO_2Cl and $SbCl_5$ (Aldrich) in dichloromethane. The slightly yellow powder of $PyNO_2^+SbCl_6^-$ was obtained by treating $NO_2^+SbCl_6^-$ with 1 equiv of pyridine in nitromethane in the manner employed for the BF_4^- salt: ^1H NMR (CD_3CN) δ 9.71 (d, 2 H, J = 7.2 Hz), 9.01 (t, 1 H, J = 7.5 Hz), 8.37 (d, 2 H, J = 7.2 Hz); IR (CH_3CN) 3123, 1723, 1610, 1207, 809, 766, 687, 659 cm^{-1}.

H. 4-$MeOPyNO_2^+SbCl_6^-$. This salt was prepared using the same procedure as described for $PyNO_2^+SbCl_6^-$: ^1H NMR (CD_3CN) δ 9.48 (dd, 2 H, J = 6.2, 2.1 Hz), 7.56 (dd, 2 H), 4.29 (s, 3 H); IR (CH_3NO_2) 3123, 1698, 1648, 1211, 845, 795, 725, 555 cm^{-1}. The reaction of NO_2SbF_6 and either pyridine or 4-methoxypyridine in acetonitrile (or nitromethane) yielded unidentified dark brown tars.

Instrumentation. The UV–vis absorption spectra were measured on a Hewlett-Packard 8450A diode-array spectrometer equipped with an HP 89100A temperature controller. The ^1H NMR spectra were recorded on a JEOL FX 90Q spectrometer operating at 90 MHz, and the proton chemical shifts are reported in ppm downfield from a tetramethylsilane internal standard. IR spectra were obtained with AgCl cells using a Nicolet 10DX FT spectrometer with 4 cm^{-1} resolution. Routine GC analyses were performed on a Hewlett-Packard 5790A chromatograph equipped with a flame ionization detector, using a 12.5-m SE-30 capillary column. For quantitative analyses, decane (Aldrich) was used as the calibration standard. Authentic nitro aromatic products were either obtained commercially or prepared according to the literature procedures.[90] The GC–MS analyses were carried out on a Hewlett-Packard

(87) See: Kim, E. K.; Kochi, J. K. *J. Am. Chem. Soc.* **1991**, *113*, 4962.
(88) The sequence in Scheme III is equivalent to the electrochemical EC process in which the (reversible) charge transfer (eq 27) is driven potentially by the followup reaction (eq 28).[77]
(89) Bouas-Laurent, H.; Castellan, A.; Desvergne, J. P. *Pure Appl. Chem.* **1980**, *52*, 2633.

5890 chromatograph interfaced to an HP 5970 mass spectrometer (EI, 70 eV). Cyclic voltammetry was performed on an IR-compensated potentiostat driven by a Princeton Applied Research (PAR) 175 universal programmer. Current–voltage curves were plotted on a Houston Series 2000 X–Y recorder or displayed on a Gould Biomation 4500 digital oscilloscope. The working electrode consisted of a platinum disk (r = 0.5 mm) embedded in glass, and a platinum gauze was used as a counter electrode. Potentials were measured relative to an SCE reference electrode ($E°$ for Cp_2Fe/Cp_2Fe^+ = 0.41 V). All manipulations of the moisture-sensitive *N*-nitropyridinium salts were carried out in a Vacuum Atmospheres HE-493 dry box maintained at <2 ppm water.

Charge-Transfer Spectral Measurements. Typically, in a 10-mm square quartz cuvette equipped with side arm and Schlenk adapter was placed 4 × 10^{-5} mol of 4-$XPyNO_2^+BF_4^-$. The cell was taken out of the dry box and connected to a vacuum line, and 1 mL of acetonitrile was added with the aid of a hypodermic syringe. An aliquot of 0.04 M arene in acetonitrile (1 mL) was carefully cannulated into the side arm of the UV cell. The cuvette was thermally equilibrated in the low-temperature bath (maintained at 0 to −40 °C with a Neslab CC-65A refrigerated thermoregulator), and the solutions were mixed. The charge-transfer absorption spectra were measured at various concentrations of 4-$XPyNO_2^+BF_4^-$ (0.02–0.05 M) and arene (0.01–0.1 M) to ensure the band maxima to be invariant and the band shapes to be homogeneous. The maxima of the charge-transfer bands in the UV region were determined by spectral subtraction of the spectra obtained with the same concentration of 4-$XPyNO_2^+BF_4^-$. For 1,4-dimethylnaphthalene, which has a relatively low energy cutoff, the maximum of the charge transfer band was determined by subtraction of the spectrum of 1,4-dimethylnaphthalene at the same concentration.

Spectrophotometric Determination of the Formation Constant. A 2-mL of aliquot of a stock solution of the *N*-nitropyridinium salt (0.02 M) in acetonitrile was placed in a UV cell. The cuvette was cooled in an ice bath, and durene was added in increments ((4–40) × 10^{-5} mol) under a positive pressure of argon as the absorbance changes were measured at 380, 400, 420, and 440 nm (where the *N*-nitropyridinium salt alone is transparent). From a plot of $[PyNO_2^+BF_4^-]/A_{CT}$ versus $[durene]^{-1}$, the slope was estimated as $\epsilon_{CT}K_{EDA}^{-1}$ and the intercept as ϵ_{CT}^{-1}.[29] The averaged formation constant, K_{EDA}, was 1.16 ± 0.07 M^{-1}, and ϵ_{CT} = 137 (380 nm), 96 (400 nm), 91 (420 nm), and 40 (440 nm) M^{-1} cm^{-1}. Each of the linear fits obtained by the least-squares method had a correlation coefficient of >0.99. The formation constant for 9-methylanthracene with $PyNO_2^+$ was determined similarly (Table II).

Aromatic Nitrations with *N*-Nitropyridinium Salts. All thermal reactions were carried out in Schlenk flasks under an inert argon atmosphere and shielded from direct room light. Preweighed amounts of *N*-nitropyridinium salts were dissolved in dry acetonitrile and mixed with arenes. Thermal reactions for X = CO_2CH_3, CN, Cl, H, and CH_3 were carried out at room temperature. The reactions of $CH_3OPyNO_2^+BF_4^-$ with alkylbenzenes were performed at elevated temperatures (50–60 °C). After stirring for certain period of time, the crude reaction mixture was first analyzed by ^1H NMR spectroscopy. The mixture was then quenched with water (or wet ether), extracted with ether, and dried over $MgSO_4$. The side chain nitrite and pyridinium products were examined by ^1H NMR spectroscopy of the reaction mixture, and others were quantified by GC and GC–MS analyses after aqueous workup as follows.

A. Toluene. To a stirred colorless solution of the *N*-nitropyridinium salt (0.076 mmol) in acetonitrile (2 mL) was added toluene (0.19 mmol) at room temperature. Initially, a bright yellow color appeared, which faded within 45 h to give a pale yellow solution. The integration of the aromatic proton resonance in the ^1H NMR spectrum with 1,2-dichloroethane as the internal standard indicated the presence of $PyH^+BF_4^-$ (0.073 mmol) and small amounts of $PyNO_2^+BF_4^-$ (0.005 mmol). Addition of ether to the reaction mixture yielded a colorless precipitate, which was identified as $PyH^+BF_4^-$ [^1H NMR (CD_3CN) δ 8.05 (t, 2 H), 8.55 (d, 1 H), 8.71 (d, 2 H)]. The organic layer, after aqueous workup, contained *o*-nitrotoluene (0.034 mmol), *m*-nitrotoluene (0.0025 mmol), and *p*-nitrotoluene (0.018 mmol), together with unreacted toluene (0.12 mmol) by GC analysis. The transient yellow solutions of toluene with 4-$NCPyNO_2^+BF_4^-$, 4-$CH_3O_2CPyNO_2^+BF_4^-$, and 4-$ClPyNO_2^+BF_4^-$ in acetonitrile were bleached within 10 min. Quantitative yields of 4-$XPyH^+BF_4^-$ were ascertained from the integration of the methyl and aromatic proton resonances in the ^1H NMR spectra of the crude reaction mixture with 1,2-dichloroethane as the internal standard: 4-$NCPyH^+BF_4^-$ ^1H NMR (CD_3CN) δ 8.37 (d, 2 H), 8.94 (d, 2 H); 4-$CH_3O_2CPyH^+BF_4^-$ ^1H NMR (CD_3CN) 4.01 (s, 3 H), 8.44 (d, 2 H), 8.9 (d, 2 H); 4-$ClPyH^+BF_4^-$ ^1H NMR (CD_3CN) 8.08 (d, 2 H), 8.71 (d, 2 H). The reaction of toluene (0.12 mmol) with 4-$CH_3OPyNO_2^+BF_4^-$ (0.048 mmol) was carried out at 50 °C for 38 h. The crude reaction mixture contained 0.028 mmol of 4-$CH_3OPyH^+BF_4^-$ and unreacted 4-$CH_3OPyNO_2^+BF_4^-$ (0.021 mmol): 4-$CH_3OPyH^+BF_4^-$ ^1H NMR (CD_3CN) δ 4.08 (s, 3 H), 7.35 (d, 2 H), 8.47 (2 H). Workup of the reaction mixture indicated the presence of *o*-nitrotoluene (0.0028 mmol), *m*-nitrotoluene (0.000 26 mmol), and *p*-nitrotoluene (0.0015 mmol), together with unreacted toluene (0.091 mmol) by GC analysis. A similar reaction was carried out with 4-$CH_3PyNO_2^+BF_4^-$ (0.049 mmol) and toluene (0.094 mmol) at room temperature for 56 h: 4-$CH_3PyH^+BF_4^-$ ^1H NMR (CD_3CN) δ 2.63 (s, 3 H), 8.56 (d, 2 H), 8.86 (d, 2 H).

B. Anisole. The initial orange color from the solution for anisole (0.18 mmol) with 4-$CH_3O_2CPyNO_2^+BF_4^-$ (0.09 mmol) in acetonitrile-d_3 faded within 1 min. The ^1H NMR spectrum of the reaction mixture indicated the presence of quantitative yields of 4-$CH_3O_2CPyH^+BF_4^-$ (0.09 mmol). The mixture, after aqueous workup, contained *o*-nitroanisole (0.061 mmol) and *p*-nitroanisole (0.025 mmol). The excess anisole was quantitatively recovered (0.094 mmol).

C. Chlorobenzene. The reaction of chlorobenzene (0.098 mmol) with 4-$CH_3OPyNO_2^+BF_4^-$ (0.060 mmol) was carried out at 60 °C for 24 h. The ^1H NMR analysis of the crude reaction mixture indicated the presence of $CH_3OPyH^+BF_4^-$ (0.018 mmol) and 4-$CH_3OPyNO_2^+BF_4^-$ (0.043 mmol), together with nitrochlorobenzenes. GC analysis of the product mixture indicated the presence of *o*-nitrochlorobenzene (0.0024 mmol), *m*-nitrochlorobenzene (0.0002 mmol), and *p*-nitrochlorobenzene (0.0057 mmol), together with unreacted chlorobenzene (0.079 mmol). A similar reaction was carried out at room temperature with 4-$CH_3O_2CPyNO_2^+BF_4^-$ in acetonitrile-d_3.

D. Bromobenzene. The pale yellow solution from the reaction of bromobenzene (0.28 mmol) and 4-$CH_3OPyNO_2^+BF_4^-$ (0.034 mmol) in acetonitrile-d_3 at 60 °C for 120 h contained 4-$CH_3OPyH^+BF_4^-$ by ^1H NMR analysis. Other products were *m*-nitrobromobenzene (0.000 13 mmol), *p*-nitrobromobenzene (0.0012 mmol), 1,4-dibromobenzene (0.0009 mmol), and 1,3-dibromobenzene (0.0001 mmol) by GC analysis. Bromobenzene (0.19 mmol) was added to a solution of 4-$CH_3O_2CPyNO_2^+BF_4^-$ (0.060 mmol) in acetonitrile. After 1 h, the mixture contained *p*-nitrobromobenzene (0.012 mmol), *m*-nitrobromobenzene (0.000 17 mmol), and 1,4-dibromobenzene (0.0006 mmol).

E. *tert*-Butylbenzene. The yellow color of the solution of *tert*-butylbenzene (0.17 mmol) with 4-$CH_3O_2CPyNO_2^+BF_4^-$ (0.084 mmol) in acetonitrile-d_3 decayed within 5 min at room temperature to a pale yellow. ^1H NMR analysis of the crude reaction mixture indicated the formation of 4-$CH_3O_2CPyH^+BF_4^-$ (0.063 mmol) together with nitrated products. The subsequent workup of the reaction mixture afforded *o*-nitro-*tert*-butylbenzene (0.01 mmol), *m*-nitro-*tert*-butylbenzene (0.012 mmol), *p*-nitro-*tert*-butylbenzene (0.063 mmol), 1,3-di-*tert*-butylbenzene (0.0001 mmol), 1,4-di-*tert*-butylbenzene (0.0002 mmol), and nitrobenzene (0.0002 mmol). The excess *tert*-butylbenzene was recovered quantitatively (0.084 mmol). Other reactions were similarly carried out at either room temperature or at 60 °C (X = CH_3O).

F. Di-*tert*-butylbenzenes. Reactions of 4-$CH_3OPyNO_2^+BF_4^-$ and 4-$CH_3O_2CPyNO_2^+BF_4^-$ with di-*tert*-butylbenzene were carried out at 60 °C and room temperature, respectively. GC analysis of the reaction mixture afforded 63–69% of ring nitration products and 31–37% of dealkylation products. The solution of 1,3-di-*tert*-butylbenzene and 4-$CH_3O_2CPyNO_2^+BF_4^-$ in acetonitrile afforded only products of ring nitration (by GC–MS analysis).

G. Mesitylene. Mesitylene (0.12 mmol) was added to a colorless solution of 4-$ClPyNO_2^+BF_4^-$ (0.056 mmol) in acetonitrile-d_3 at room temperature. The yellow color from the initial mixing faded within 2 min, and the solution afforded nitromesitylene (0.055 mmol) and 4-$ClPyH^+BF_4^-$ (0.051 mmol) by ^1H NMR analysis. Analogous reactions with other *N*-nitropyridinium salts also afforded nitromesitylene (Table VII).

H. Naphthalene. Naphthalene (0.05 mmol) was dissolved in acetonitrile (1 mL) under an argon atmosphere, and the solution was added to 4-$CH_3O_2CPyNO_2^+BF_4^-$ (0.094 mmol) in acetonitrile (1 mL) at room temperature. Initially, an orange color appeared which faded within 2 min to give a pale yellow solution. Workup of the reaction mixture afforded 1-nitronaphthalene (0.038 mmol) and 2-nitronaphthalene (0.007 mmol) by GC analysis.

I. Durene. Durene (0.085 mmol) was added to the solution containing 4-$CH_3O_2CPyNO_2^+BF_4^-$ (0.04 mmol) at room temperature. The initial orange color bleached within 2 min. The characteristically structured UV band of the nitrite product was observed at 350–400 nm, and ^1H NMR analysis of the reaction mixture indicated the presence of 2,4,5-

(90) (a) Bewick, A.; Edwards, G. J.; Mellor, J. M.; Pons, S. *J. Chem. Soc., Perkin Trans. 2* **1977**, 1952. (b) Eberson, L.; Nyberg, K. *Tetrahedron Lett.* **1966**, 2389. (c) Kim, E. K.; Kochi, J. K. *J. Org. Chem.* **1989**, *54*, 1692. (d) Schlesener, C. J.; Kochi, J. K. *J. Org. Chem.* **1984**, *49*, 3142. (e) Gonzales, A. G.; Aguiar, J. M.; Martin, J. D.; Rodriguez, M. L. *Tetrahedron Lett.* **1976**, 205. (f) Suzuki, H. *Nippon Kagaku Kaishi* **1978**, 7, 1049. (g) Masnovi, J. M.; Sankararaman, S.; Kochi, J. K. in ref 83.

trimethylbenzyl nitrite (0.011 mmol), (2,4,5-trimethylphenyl)nitromethane (δ 5.43 in $CDCl_3$), and $CH_3O_2CPyH^+BF_4^-$. Other products were 3-nitrodurene (0.0023 mmol), 2,4,5-trimethylbenzyl alcohol (0.0036 mmol), (2,4,5-trimethylbenzyl)acetamide (0.0069 mmol), and 2,2',3',4,5,5',6'-heptamethyldiphenylmethane (0.0007 mmol)[90] by GC analysis. The authentic 2,4,5-trimethylbenzyl nitrite was obtained from the reaction of 2,4,5-trimethylbenzyl chloride and silver nitrite at room temperature: ^1H NMR ($CDCl_3$) δ 5.70 (s, 2 H). 2,4,5-Trimethylbenzyl nitrite decomposed at 60 °C within 16 h to give 2,4,5-trimethylbenzaldehyde and 2,4,5-trimethylbenzyl alcohol.

J. Pentamethylbenzene. Pentamethylbenzene (0.15 mmol) was added to a solution of $4\text{-}CH_3O_2CPyNO_2^+BF_4^-$ (0.075 mmol) at room temperature. The initial orange color bleached within 5 min to a colorless solution which afforded tetramethylbenzyl nitrite (δ 5.65, 0.022 mmol), (tetramethylphenyl)nitromethane (δ 5.45 and 6.99), and a quantitative yield of $4\text{-}CH_3O_2CPyH^+BF_4^-$ by ^1H NMR analysis. The organic layer, after aqueous workup of the reaction mixture, contained nitropentamethylbenzene (0.0096 mmol), (tetramethylphenyl)nitromethane (0.022 mmol), *N*-(tetramethylbenzyl)acetamide (0.011 mmol), and nonamethyldiphenylmethane (0.013 mmol) by GC analysis. Other reactions were carried out in a similar manner (Table VII).

K. Hexamethylbenzene. Hexamethylbenzene (0.095 mmol) was added to a colorless solution of $4\text{-}NCPyNO_2^+BF_4^-$ (0.084 mmol) in acetonitrile-d_3 at room temperature. The transient red color from the initial mixing disappeared within a few seconds. The product mixture contained *N*-(pentamethylbenzyl)-4-cyanopyridinium tetrafluoroborate (0.039 mmol), which was identified by its characteristic methylene proton resonance at δ 5.93, pentamethylbenzyl nitrite (0.011 mmol at δ 5.78), and (pentamethylphenyl)nitromethane (0.003 mmol) at δ 5.71, together with $4\text{-}NCPyH^+BF_4^-$ by ^1H NMR analysis. Examination of the organic layer after aqueous workup indicated the presence of *N*-(pentamethylbenzyl)acetamide (0.011 mmol), as well as the nitro and nitrite products described above. The orange color of the hexamethylbenzene (0.12 mmol) with $4\text{-}CH_3OPyNO_2^+BF_4^-$ (0.09 mmol) bleached at 60 °C after 1 day. The ^1H NMR spectrum of the reaction mixture indicated the presence of $4\text{-}CH_3OPyH^+BF_4^-$ (0.09 mmol), pentamethylbenzyl nitrite (0.012 mmol), (pentamethylbenzyl)nitromethane (0.016 mmol), *N*-(pentamethylbenzyl)acetamide (0.022 mmol), and pentamethylbenzyl alcohol (0.018 mmol) at δ 4.75 by ^1H NMR integration.

L. Hexamethyl(Dewar benzene), HMDB, (0.25 mmol) was added to a solution of $PyNO_2^+BF_4^-$ (0.024 mmol) in 2 mL of acetonitrile. A yellow color developed upon stirring at room temperature for 100 min. Workup of the solution afforded 18 mg of hexamethylbenzene (475% based on $PyNO_2^+$), and the unreacted HMDB was 0.064 mmol by GC analysis. A solution of HMDB (0.021 mmol) with $4\text{-}CH_3OPyNO_2^+BF_4^-$ (0.21 mmol) in 2 mL of acetonitrile was stirred at room temperature. The yellow color of the CT complex of HMB and $4\text{-}CH_3OPyNO_2^+BF_4^-$ developed upon standing at room temperature for 5 days. [The observed pseudo-first-order rate constant was 5×10^{-6} s^{-1}.] Workup of the reaction mixture afforded hexamethylbenzene (0.013 mmol).

M. 9-Methylanthracene dimer, MA_2, (0.047 mmol) in 40 mL of dichloromethane was added to a Schlenk flask charged with $4\text{-}CH_3O_2CPyNO_2^+BF_4^-$ (0.047 mmol) in 2 mL of acetonitrile at room temperature. The colorless mixture was stirred for 1 h to give a yellow solution. The formation of 9-methylanthracene was indicated by its electronic absorption spectrum. The solution was washed with water, concentrated in vacuo, and subjected to thin-layer chromatography using hexane as an eluent. 9-Methylanthracene (0.005 mmol) separated as the initial TLC fraction. Similarly, MA_2 (0.055 mmol) was treated with $PyNO_2^+BF_4^-$ (0.054 mmol) in a mixture of dichloromethane and acetonitrile. After 8 h at room temperature, 9-methylanthracene (0.005 mmol, 9%) was isolated from the first TLC fraction. Other products appeared to be a mixture of products of 9-methylnitroanthracene. To a well-stirred solution of MA_2 (0.064 mmol) in 5 mL of dichloromethane was added a solution of $NO_2^+BF_4^-$ (0.057 mmol) in 1 mL of acetonitrile. The vivid green color of the radical cation of 9-methylanthracene (694, 640, 580, and 440 nm) was observed upon mixing. Aqueous workup of the green solution mixture led to the discharge of the color, and it yielded 9-methylanthracene (0.007 mmol) by TLC analysis.

N. 2,3-Bis(trimethylsiloxy)-2,3-diphenylbutane (d, l and meso mixture, 0.043 mmol) or P_2 was added to a colorless solution of $4\text{-}CH_3O_2CPyNO_2^+BF_4^-$ (0.041 mmol) in acetonitrile-d_3 at room temperature. The initial yellow color bleached within 10 min. The ^1H NMR spectrum of the crude mixture indicated the presence of acetophenone (δ 2.5), $4\text{-}CH_3O_2CPyH^+BF_4^-$, unreacted P_2 (δ −0.15, 0.04, 1.36, 1.75, 6.9, 7.2, 7.7), and other unknown pyridinium and TMS derivatives (δ 0.083, 0.16, 0.25, and 3.98) and other products (δ 1.4 and 1.8). After aqueous workup, the yields of acetophenone and P_2 were found to be 0.0043 mmol and 0.01 mmol, respectively, by GC analysis. Other products (0.006 mmol) were the ring-nitrated products, $(NO_2)C_6H_4[C(CH_3)OTMS]_2C_6H_5$, by GC–MS analysis [*m/e* 416 (0.8), 370 (2.3), 194 (15), 193 (92), 73 (100)]. The reaction of P_2 with $PyNO_2^+BF_4^-$ (0.047 mmol) was carried out at room temperature. Initially, the color of the solution was pale yellow, which turned to yellow upon standing at room temperature. Within 30 min, no reaction was apparent by ^1H NMR analysis. After 4 days at room temperature, the product mixture contained acetophenone, $PyH^+BF_4^-$, and other (unidentified) products (δ −0.18, 0.03, 0.14, 0.22, 1.07, 1.85, 2.04). The subsequent aqueous workup of the reaction mixture indicated the presence of acetophenone (0.009 mmol, 19%) and unreacted P_2 (0.018 mmol). A mixture of nitrated products, $(NO_2)C_6H_4[C(CH_3)OTMS]_2C_6H_5$ (0.004 mmol), was also observed, together with 1,1-diphenylethyl methyl ketone (0.005 mmol) by GC–MS analysis [*m/e* 224 (0.03), 208 (0.01), 181 (100), 103 (43), 77 (28)].

O. Dicumene, $[C_6H_5C(CH_3)_2]_2$, was examined as follows. The nitration of dicumene (0.019 mmol) with $4\text{-}CH_3O_2CPyNO_2^+BF_4^-$ (0.099 mmol) in 2 mL of acetonitrile was complete after 10 min. Aqueous workup of the reaction mixture afforded 0.01 mmol of a mixture of nitrodicumenes (M^+, 281, 119), together with unreacted dicumene (0.004 mmol) by GC and GC–MS analyses. The reaction of dicumene (0.056 mmol) with $PyNO_2^+BF_4^-$ (0.094 mmol) in acetonitrile-d_3 was carried out at room temperature for 17 h. The product mixture contained a mixture of nitrodicumenes (0.01 mmol) and unreacted dicumene (0.023 mmol) by GC analysis. Dicumene (0.5 mmol) was added to a solution containing 1 mmol of $NO_2^+BF_4^-$ in 2 mL of acetonitrile. The reaction mixture after 5 min contained nitrodicumenes (50%) and dinitrodicumenes (7%), together with unreacted dicumene by GC and GC–MS analyses.

Rates and Kinetics of Aromatic Nitration. The rates of reaction between *N*-nitropyridinium cation and various arenes were followed spectrophotometrically by monitoring the disappearance of the charge-transfer absorption bands at selected wavelengths (Table VIII). All of the reactions were carried out in a 1.0-cm quartz cuvette (fitted with a Teflon stopcock) in the dark at 23 °C, and their course was followed to greater than 90% completion. Typically, an aliquot of 0.02 M *N*-nitropyridinium salt in 1–2 mL of acetonitrile in the side arm of the UV cell was added to a solution containing the arene (0.10–2.5 M) in 2–5 mL of acetonitrile. The initial absorption spectrum was measured after 5 s (mixing time). The pseudo-first-order rate constant k_{obsd} was obtained from the least-squares evaluation of the slope of the absorbance change $\ln (A_t - A_0)$ with time, where A_t and A_0 are the absorbances of the CT band at time t and final time, respectively. In all cases, the fitting in the pseudo-first-order plots occurred with a correlation coefficient of 0.995 or better. The pseudo-first-order rate constants were independent of the monitoring wavelength. The kinetics studies were carried out at various concentrations of arenes for the reactions of toluene with $4\text{-}MeO_2CPyNO_2^+BF_4^-$ and of 9-methylanthracene with $PyNO_2^+BF_4^-$. The kinetics measurement of benzene (0.022 M) with $4\text{-}MeO_2CPyNO_2^+BF_4^-$ (0.23 M) was followed spectrophotometrically by monitoring the formation of product bands at 360, 370, and 380 nm. The kinetics measurement of mesitylene (0.25 M) and $PyNO_2^+BF_4^-$ (0.025 M) in acetonitrile was also followed by measuring the formation of nitromesitylene by GC analysis.

The relative rates of reaction of various arenes with N-nitropyridinium cations were determined by the competition method similar to that described by Olah, Stock, and co-workers.[91] Aliquots of $4\text{-}CH_3O_2CPyNO_2^+BF_4^-$ (0.02–0.045 M) in acetonitrile (1–3 mL) were added to a well-stirred solution of a mixture of benzene and toluene (0.4–2.1 M) at 23 °C. After 2–10 min, the reaction mixture was quenched with ice-cold water, extracted with ether, dried with $MgSO_4$, and subjected to GC analysis. The ratios of nitrotoluenes (*o*, *m*, *p*) to nitrobenzene were 7.6, 12.4, 27, 49, and 121 when the concentrations (M) of [toluene, benzene] were [0.45, 2.13], [0.47, 1.15], [0.41, 0.42], [0.90, 0.55], and [1.79, 0.55], respectively. When the mixture of benzene (0.42 M) and toluene (0.41 M) in 2 mL of acetonitrile reacted with $4\text{-}CH_3O_2CPyNO_2^+BF_4^-$ (0.073 mmol) at −5 °C for 30 s, the corresponding ratio of nitrotoluenes to nitrobenzene was 31 at 9.5% conversion. Similarly, aliquots of *N*-nitropyridinium salt (0.025 M) were added to a well-stirred solution of benzene and toluene in acetonitrile at room temperature. After 3–5 h, the reaction mixture was quenched, and ratios of nitrotoluenes:benzene were 6.8, 13, 31, 53, and 131 when the concentrations (M) of arene [toluene, benzene] were [0.45, 2.13], [0.47, 1.15], [0.41, 0.42], [0.90, 0.55], and [1.79, 0.55], respectively. The relative rate k/k_0 for $4\text{-}NCPyNO_2^+BF_4^-$ was obtained at −40 °C by addition of the solution of benzene (2.13 M) and toluene (0.45 M) to a solution of $4\text{-}NCPyNO_2^+BF_4^-$ (0.023 M) in acetonitrile. The ratio of nitrotoluenes to benzene was 10, which corresponded to a k/k_0 ratio of

(91) (a) Olah, G. A.; Overchuk, N. A. *Can. J. Chem.* **1965**, *43*, 3279. (b) Stock, L. M.; Brown, H. C. *Adv. Phys. Org. Chem.* **1963**, *1*, 35.

48.

Other competition reactions were similarly carried out at either room temperature or 60 °C (4-$CH_3OPyNO_2^+BF_4^-$). The relative rate, k/k_0, was obtained from the plot of the ratios of nitro products against ratios of arenes. The normalized and averaged k/k_0 values were 48, 33 ± 5, 26, 36 ± 5, 25, and 24 when the X substituents on $XPyNO_2^+BF_4^-$ were CN (at −40 °C), CO_2CH_3, Cl, H, CH_3, and OCH_3 (at 60 °C), respectively. The relative reactivities of other arenes were determined similarly. Thus, the [arene mixture] and normalized relative reactivities were as follows: [mesitylene, anisole], 1.4; [mesitylene, *m*-xylene], 4.4; and [mesitylene, toluene], 89 for 4-$CH_3O_2CPyNO_2^+BF_4^-$. The relative reactivities for $PyNO_2^+BF_4^-$ were [mesitylene, toluene], 130 and [mesitylene, *m*-xylene], 6.4 at room temperature. Cold aliquots (−42 °C) of $NO_2^+BF_4^-$ (0.012–0.09 M) in 2 mL of acetonitrile were added to a well-stirred solution of toluene and benzene (0.14–0.9 M) in 8 mL of acetonitrile at −42 °C with the aid of either a cannula or jacketed dropping funnel. The precooled solution of pyridine in either (−50 °C) was added to quench the reaction after 1–10 min. Addition of water followed, and the mixture was warmed to 0–5 °C. The mixture was extracted with ether after the addition of decane (internal standard), and the etheral solution was subjected to GC analysis. The ratios of nitrotoluenes:nitrobenzene were 3.1, 8.6, 8.3, 21, 41.5, and 67.4 when arene concentrations [toluene, benzene] were [0.14, 0.90], [0.14, 0.50], [0.14, 0.39], [0.14, 0.17], [0.30, 0.17], and [0.42, 0.17], respectively. The normalized k/k_0 value was 25 ± 5. When the mixing of $NO_2^+BF_4^-$ with arene was uncontrolled, the value of k/k_0 was considerably lower. Thus the solution of $NO_2^+BF_4^-$ (0.026 mmol) in 2 mL of acetonitrile (−32 °C) was added to the solution of toluene (0.28 M) and benzene (0.34 M) in 8 mL of acetonitrile at −32 °C. The solution was allowed to stand for 8.5 min without stirring at −32 °C. The ratio of nitrotoluene:nitrobenzene was 1.6, which was corresponded to a k/k_0 value of 1.8. Similarly, when the solution of $NO_2^+BF_4^-$ (0.036 M) in acetonitrile was added to a stirred solution of toluene (0.41 M) and benzene (0.42 M) at room temperature, the ratio of nitrotoluenes:nitrobenzene was 1.3. The relative reactivities of mesitylene and toluene toward $NO_2^+BF_4^-$ were similarly examined at −42 °C. The solution of $NO_2^+BF_4^-$ (0.045 M) in 1 mL of acetonitrile at −42 °C was added to a well-stirred solution of mesitylene (0.19 M) and toluene (0.9 M) in acetonitrile at −42 °C. The ratio of nitromesitylene:nitrotoluenes after 2 min was 1.24, which corresponded to a k_m/k_t value of 5.92. No dinitration product was observed in this experiment. The relative ratios of nitration products (k_m/k_t) were 3.4 (2.9), 1.53 (3.8), and 3.46 (4.5) when arene concentrations (M) of [mesitylene, toluene] were [0.21, 0.18], [0.28, 0.11], and [0.14, 0.11], respectively. The averaged value of k_m/k_t was 4.3 from these experiments. For the correlation in Figure 10B, the value of $k_2 = 10^{-5}$ M^{-1} s^{-1} was arbitrarily set for benzene nitration with $PyNO_2^+$, and $k_2 = 3.6 \times 10^{-4}$, 7.3×10^{-3}, and 4.7×10^{-2} M^{-1} s^{-1} was obtained for toluene, *m*-xylene, and mesitylene on the basis of k/k_0 = 36, 730, and 4700, respectively. Similarly, the value of $k_2 = 7.8 \times 10^{-5}$ M^{-1} s^{-1} was calculated for benzene nitration with $MeO_2CPyNO_2^+$ on the basis of the LUMO difference of $\Delta E_p^c = 0.21$ V for $PyNO_2^+$ and $MeO_2CPyNO_2^+$ in Table III and the correlation described above; $k_2 = 2.5 \times 10^{-3}$, 5.5×10^{-2}, and 2.3×10^{-1} M^{-1} s^{-1} was obtained for toluene, *m*-xylene, and mesitylene on the basis of k/k_0 = 33, 700, and 3000, respectively. At room temperature, the solution of $NO_2^+BF_4^-$ (0.075 mmol) in 2 mL of acetonitrile was added to a solution of mesitylene (0.76 mmol) and toluene (10.8 mmol) in 4 mL of acetonitrile. Immediately after mixing, an orange color developed and it was discharged by quenching with pyridine after 2 min. The product mixture contained nitromesitylene, nitrotoluenes, and dinitromesitylene (M^+, 210, 5% yield) by GC and GC–MS analyses. The normalized value of k_m/k_t was 0.90. The reaction of $NO_2^+BF_4^-$ with arene mixtures in butyronitrile at −65 °C was difficult to control owing to the precipitation of $NO_2^+BF_4^-$ and the nitration product at −65 °C. The reaction of $NO_2^+BF_4^-$ with arene in dichloromethane was similarly difficult.

To a well-stirred solution of 4-$MeO_2CPyNO_2^+BF_4^-$ (0.019 mmol) in 1 mL of acetonitrile was added a solution of toluene-d_8 (0.19 mmol) and toluene (0.18 mmol) in acetonitrile (1 mL) at room temperature. After 30 s of stirring, the reaction mixture was quenched with water and analyzed by GC and GC–MS. The area ratio for the deuterated and protiated nitro products (total conversion 12%) afforded a k_H/k_D value (normalized) of 0.91.

Acknowledgment. We thank the National Science Foundation, Robert A. Welch Foundation, and Texas Advanced Research Program for financial assistance.

Registry No. HMDB, 7641-77-2; 1,2,3,5-$(CH_3)_4C_6H_2$, 527-53-7; $(CH_3)_5C_6H$, 700-12-9; 4-$MeO_2CPyNO_2^+BF_4^-$, 138333-61-6; $PyNO_2^+BF_4^-$, 2375-72-6; 4-$MeOPyNO_2^+BF_4^-$, 138333-63-8; 4-$MePyNO_2^+BF_4^-$, 138333-65-0; 4-$NCPyNO_2^+BF_4^-$, 138333-67-2; 4-$ClPyNO_2^+BF_4^-$, 138333-69-4; $NO_2^+BF_4^-$, 13826-86-3; Py, 110-86-1; 4-MeOPy, 620-08-6; 4-ClPy, 626-61-9; 4-NCPy, 100-48-1; $[C_6H_5C(CH_3)_2]_2$, 1889-67-4; ClC_6H_5, 108-90-7; BrC_6H_5, 108-86-1; $CF_3C_6H_5$, 98-08-8; *t*-BuC_6H_5, 98-06-6; (4-$MeOPyNO_2^+BF_4^-$)·mesitylene, 138353-17-0; (4-$MeOPyNO_2^+BF_4^-$)·durene, 138333-70-7; (4-$MeOPyNO_2^+BF_4^-$)·pentamethylbenzene, 138333-71-8; (4-$MeOPyNO_2^+BF_4^-$)·hexamethylbenzene, 138333-72-9; (4-$MeOPyNO_2^+BF_4^-$)·1,4-dimethylnaphthalene, 138333-73-0; (4-$MeOPyNO_2^+BF_4^-$)·9-methylanthracene, 138333-74-1; (4-$MeOPyNO_2^+BF_4^-$)·9,10-dimethylanthracene, 138333-75-2; (4-$MePyNO_2^+BF_4^-$)·mesitylene, 138333-76-3; (4-$MePyNO_2^+BF_4^-$)·durene, 138333-77-4; (4-$MePyNO_2^+BF_4^-$)·pentamethylbenzene, 138333-78-5; (4-$MePyNO_2^+BF_4^-$)·hexamethylbenzene, 138333-79-6; (4-$MePyNO_2^+BF_4^-$)·1,4-dimethylnaphthalene, 138333-80-9; (4-$MePyNO_2^+BF_4^-$)·9-methylanthracene, 138333-81-0; (4-$MePyNO_2^+BF_4^-$)·9,10-dimethylanthracene, 138333-82-1; ($PyNO_2^+BF_4^-$)·mesitylene, 138333-83-2; ($PyNO_2^+BF_4^-$)·durene, 138333-84-3; ($PyNO_2^+BF_4^-$)·pentamethylbenzene, 138333-87-6; ($PyNO_2^+BF_4^-$)·hexamethylbenzene, 133586-10-4; ($PyNO_2^+BF_4^-$)·1,4-dimethylnaphthalene, 133586-09-1; ($PyNO_2^+BF_4^-$)·9-methylanthracene, 133586-11-5; ($PyNO_2^+BF_4^-$)·9,10-dimethylanthracene, 133586-18-2; (4-$ClPyNO_2^+BF_4^-$)·mesitylene, 138333-85-4; (4-$ClPyNO_2^+BF_4^-$)·durene, 138333-86-5; (4-$ClPyNO_2^+BF_4^-$)·pentamethylbenzene, 138333-88-7; (4-$ClPyNO_2^+BF_4^-$)·hexamethylbenzene, 138333-89-8; (4-$ClPyNO_2^+BF_4^-$)·1,4-dimethylnaphthalene, 138333-90-1; (4-$ClPyNO_2^+BF_4^-$)·9-methylanthracene, 138333-91-2; (4-$ClPyNO_2^+BF_4^-$)·9,10-dimethylanthracene, 138333-92-3; (4-$MeO_2CPyNO_2^+BF_4^-$)·mesitylene, 138333-93-4; (4-$MeO_2CPyNO_2^+BF_4^-$)·durene, 138333-94-5; (4-$MeO_2CPyNO_2^+BF_4^-$)·pentamethylbenzene, 138333-95-6; (4-$MeO_2CPyNO_2^+BF_4^-$)·hexamethylbenzene, 138333-96-7; (4-$MeO_2CPyNO_2^+BF_4^-$)·1,4-dimethylnaphthalene, 138333-97-8; (4-$MeO_2CPyNO_2^+BF_4^-$)·9-methylanthracene, 138333-98-9; (4-$MeO_2CPyNO_2^+BF_4^-$)·9,10-dimethylanthracene, 138333-99-0; benzene, 71-43-2; toluene, 108-88-3; mesitylene, 108-67-8; 9-methylanthracene, 779-02-2; *p*-xylene, 106-42-3; durene, 95-93-2; hexamethylbenzene, 87-85-4; methyl isonicotinate, 2459-09-8; naphthalene, 91-20-3; *m*-xylene, 108-38-3; 1,3-di-*tert*-butylbenzene, 1014-60-4; 1,4-di-*tert*-butylbenzene, 1012-72-2; 2,3,5-trimethylbenzyl nitrate, 119296-66-1; 2,3-bis(trimethylsiloxy)-2,3-diphenylbutane, 21081-92-5.